SLAC-PUB-528
December 1968
(EXP) & (EXPI)

RECENT DEVELOPMENTS IN THE DESIGN OF SUPERCONDUCTING MAGNETS*

H. Brechna

Stanford Linear Accelerator Center
Stanford University
Stanford, California

I. INTRODUCTION

Electromagnets as an experimental tool in physics have occupied a significant position. With the increasing sophistication in all areas of physics, requirements on magnets, such as field strength, field distribution, optical properties, have been increasing steadily. The discovery of superconductors type II made most of the new requirements feasible.

Superconducting magnets can be found readily in all areas of science. Progress in the last few years has been remarkable. A paper covering all the important developments of only the last two to three years is hardly readable. Ignoring achievements may prove fatal. A compromise solution is suggestive but dangerous, because it is subjective. After some reflection, I finally decided to discuss some important achievements in more detail and refer to literature for others, which will be beyond the scope of a concise paper.

Reliable utilization of magnets in high-energy physics would not be possible without the progress in superconducting materials and, therefore, their main features will be discussed in some depth.

---

*Work supported by the U. S. Atomic Energy Commission

(Invited paper, presented at the 1968 Fall Meeting of the American Physical Society, Miami Beach, Florida, November 1968)

The paper will discuss conductors widely used for dc and ac applications; it will devote a section to medium-size solenoids and Helmholtz configurations, and to beam transport and large experimental magnets. Proposed magnets are mentioned only if they provide new aspects, or indicate major progress in the area of superconductivity, or may be essential for the success of an experimental endeavor.

Since the discovery of Nb_3Sn, superconducting magnets have been used in solid-state physics, magneto-optical experiments, NMR, but their progress in high-energy physics has been slow. This has been due mainly to economic reasons, safety requirements, reliability, field reproducibility, and others. This paper tries to show that superconducting magnets are as reliable as water-cooled magnets, which have been used for decades in many areas of physics, and in high-energy physics since large accelerators became reality.

II. SUPERCONDUCTING TYPE II MATERIALS AND COMPOSITE CONDUCTORS

We consider specifically type II superconductors, which are commercially available and have been shaped and processed into various types of magnet conductor, such as Nb_xTi and Nb_3Sn. Other type II materials--binary systems such as V_3Ga, ternary systems such as $Nb_{12}Al_3Ge_1$, $Nb_xTi_yTa_z$, $Nb_xTi_yZr_z$, etc.--have attractive features such as a critical field in excess of 22 T at temperatures above 10° K and transition temperature up to 20.98° K, but at present they are not available in conductor form and in practical, useful lengths, or are brittle, have low pinning strength and not suitable for current transportation. Additional research work is indicated to improve the current-carrying capacity of these alloys.

Superconductor alone cannot be used as a conductor; it requires the backing of a low electrical resistivity and high thermal conductivity normal metal,

simply because it is difficult to maintain isothermal conditions in the conductor while changing the magnetic field. Magnetic field variation at the conductor may occur either while charging or discharging the magnet, or due to external or internal disturbances of short or long duration. The magnetic flux can diffuse faster through the bulk superconductor than can the heat generated by the moving flux. This condition is seen readily from magnetic and thermal diffusion equations, considered by Swartz-Bean[1] and Wipf.[2] Quantitative diffusion data for some alloys type II are given by Brechna,[3] and show that at 4.2° K, the magnetic diffusivity in Nb_3Sn is 10...15 cm^2/sec at a field change of 1 T/sec, compared to a thermal diffusivity of 0.37 cm^2/sec.

The superconductor is heated appreciably if a sudden field change occurs. Recalling the fact that the critical current density of a high-field superconductor decreases with increasing temperature, the field penetration depth in the conductor, which is inversely proportional to the critical current density, increases. Thus a temperature rise leads to a further field penetration, which again leads to a heating effect and further field penetration, etc. We may speak of a so-called thermomagnetic feedback which, under unfavorable conditions, can lead to a thermal instability or a fluxjump, which may destroy superconductivity and yield a region of normality. As the resistivity of high-field superconducting alloy in a normal state is in the order of 5×10^{-4} ohm · cm, the joule heating may be excessive and destroy the conductor.

Even when the applied field (or transport current in the conductor) is increased relatively slowly, flux penetrates the sample in jumps. Local flux fluctuations at random may grow to gross fluxjumps, and again the process of flux and heat diffusion takes place.

Three possible methods have been investigated, which are mentioned below:

- Reducing the size of individual superconductors such that at certain lower size limits, no fluxjump will occur. In this case, the diameter of individual superconducting filaments will be less than 2.5×10^{-3} cm.

- Utilizing the heat capacity of the coil (adiabatic or enthalpy stabilization). This is possible by utilizing helium in close proximity to individual filaments or introducing normal materials (i.e., Pb) having heat capacities higher than that of the superconductor.
- Using adequate amounts of low-resistivity normal metal in good thermo-electrical contact with the superconductor. Thus ample amounts of copper or aluminum must be used in conjunction with the superconductor.

As the third solution was the easiest to achieve, the so-called "composite conductor" was introduced. In the simplest form, the composite conductor comprises a number of superconducting filaments (Nb_xTi or Nb_xZr), roped together with copper wires and impregnated with either indium or a silver-tin alloy, as shown in Fig. 1. This "cable" is readily available in lengths of several hundred meters, is flexible and inexpensive; however, it does not have the features of composites produced by drawing or swaging filaments in a copper or aluminum matrix, as illustrated in Fig. 2 and 3.

Nb_3Sn is available in the form of composite tapes. The tapes consist either of a Hastelloy (molybdenum-nickel-stainless steel) substrate, vapor-deposited Nb_3Sn (on both sides of the substrate), and subsequently copper- or silver-plated; or of a niobium substrate coated with tin, silver-plated and subsequently soldered to copper strips for stabilization and reinforced with stainless steel ribbons. Figure 4 illustrates schematically such a tape.

The normal low-resistivity metal increases the thermal diffusivity of the composite conductor by several orders of magnitude, such that for a stable conductor $D_{th} > D_{flux}$. The heat generated in the superconductor is absorbed by the normal metal and conducted to the coolant.

Composite conductors with fine filaments are also available commercially. In the absence of fluxjumps, the amount of normal metal in conjunction with the

superconductor is less than in the previous case. Copper-to-superconductor volume ratio of 1:1 is currently being used for small- and medium-size magnets.

Enthalpy-stabilized conductors with high heat capacity are somewhat harder to come by, due to difficulties in producing such conductors in long lengths. Conductors with a lead matrix[4] and porous conductors[5] to allow helium gas to penetrate the conductor are being investigated.

With stabilized conductors, short-sample critical current in coils is generally achievable. However, there are limitations in the overall operational current densities in conductors being wound into a coil. While in small-size coils (field energies less than 10^6 joules) and transverse field at the conductor of ~ 6 T, overall current densities in the conductor of $\sim 5 \times 10^4$ A/cm^2 are readily achievable, the current density is limited in large coils by the acting Lorentz force. Thus current density in the conductor seldom exceeds 1.5×10^4 A/cm^2. In most cases, the use of additional reinforcing strips (stainless steel or 2.5% Be-Cu) is imperative to prevent conductor movements beyond its elastic limit, which may lead to a loose coil structure after repeated operations, or work-hardening of the normal metal matrix.

In composite conductors, not utilizing extra-fine filaments, which are preferred for dc applications due to lower costs, heat generated by fluxjumps must be carried away by the coolant. Helium can absorb, in the nucleate boiling region, about 0.8 W/cm^2 on the surface of the conductor (unrestricted flow). However, in most magnets built, the surface heat flux has not exceeded 0.4 W/cm^2. Figure 5 gives heat flux data measured in small coils by Whetstone.[6]

If superfluid is utilized to cool down coils and keep the coil temperature below the λ-point, higher heat flux values are generally achievable (Fig. 6). While coils wound with Nb_xTi cables cooled to 1.9° K have not shown a marked improvement in overall current field performance, measurements of compactly wound coils with

Nb_3Sn tapes show a marked performance improvement, while the magnetic critical field could be boosted up 40% from values measured at 4.2° K.

In conductors utilizing filament sizes according to the simple rule of

$$d_f J_c \leqq 1500 \text{ A cm}^{-1}$$

where no fluxjumps may occur, helium plays only the role of maintaining the conductor temperature. Coils built with these conductors do not require close helium proximity and thus may be potted in a rigid thermoset, which eliminates any wire movements. For high-precision coils, where any wire movements result in a small field inhomogeneity, this type of conductor may be useful.

As the overall H-J behavior of high field superconductors from short-length test, with no helium-flow restriction, and the behavior of these conductors in coils, are of interest, Fig. 7 illustrates H-J characteristics of a few superconductors. While Nb_xZr is no longer in use, Nb_xTi alloys are generally used up to fields of 7 T in magnets and Nb_3Sn at higher fields.

Finally, Fig. 8 gives the price per ampere-meter of simple conductor configurations.[7] For complicated composite conductors, these prices are not indicative.

In addition to the cost of superconducting magnets, one must consider the cost of the refrigerator, which is used for cool-down and operation of magnets. Figure 9 gives a crude price estimate of the refrigerator system as a function of output cooling power.

The radio of refrigeration output power to installed power[8] is given in Fig. 10.

III. SUPERCONDUCTING SOLENOIDS AND AXIALLY SYMMETRIC SYSTEMS

High-field solenoids and Helmholtz configurations have been available for some time. Their geometry, simple support and cooling mechanisms have made it possible that, since 1964, many high-field magnets with field energies less than 10^6 joules have been used for physics experiments, in biology, chemistry, and other areas. Since 1966, several magnets with field energies in excess of 10^6 joules have been tested and most of these magnets are now useful tools for testing materials, for bubble-chamber experiments, MHD power generation and thermonuclear controlled fission and plasma work.

In stabilized magnets, the conductor price is about 30 - 40% of the total capital cost of equipment. In large magnets, the conductor price is a major amount. To optimize the coil capital cost, one can minimize the amount of superconducting materials and substrate by utilizing the J_c and ρ_n (resistivity of the normal metal) dependency on the magnetic field. By careful mapping of the field over the entire coil cross section, one may vary the amount of superconductor and substrate as a function of the total field. This is accomplished either by dividing the coil cross-sectional area into appropriate zones (modules), each being current-optimized, or varying the amount of superconductor and substrate within a continuous conductor length, or energizing the coil from various current sources. If each module is mechanically self-supporting, magnetomechanical forces are much easier to handle also.

Parallel to the development of multisectional coils, much attention has been given to optimizing current leads. The basic objective is to prevent heat conduction from the warm end of the lead to the cold end into the magnet and helium bath. Current leads are necessary in large magnets to energize the coils and in case of a major breakdown, dissipate the field energy into external resistors. Leads up to 10^4 A, based on counter-flow cooling, utilizing the latent heat of helium gas, are developed with loss factors

ranging down to 10^{-3} W/A/lead maximum rated current level. Ideas to lift the leads when the coil is energized, after disconnecting them from the coil, above the helium level to reduce further heat conduction are pursued. In this case, a fluxpump will maintain field amplitude and correct any small current fluctuations. Energy dissipation into external low-inductance resistors has been successfully performed up to 6 Mj, where about 90% of the total field energy could be dissipated externally and helium could be preserved. For slow variation of current, additional shunts and diodes are used in parallel to the current source, protecting the low-voltage power supply and varying slowly the magnet current until superconducting conditions are restored.

From an array of magnets, I have selected a few which are discussed in detail. Several others are mentioned in the literature cited. The list presented here is by no means complete.

(a) RCA-NASA 15-T Solenoid

A superconducting solenoid to generate fields up to 15 T in a bore 3.7 cm in diameter, length of 18 cm, and overall diameter of 31.5 cm, was recently tested by RCA.[9] It has an inductance of 90 H and a field energy of 0.8 Mj. The conductor is a 2.25-mm wide Nb_3Sn tape, stabilized by means of copper strips and silver. The magnet requires a charging time of 45 minutes. To reduce magnetomechanical stresses in the conductor, the coil is divided into four self-supporting modules, which can slip on each other axially. This magnet, built for NASA, has produced to date the highest field ever generated by a superconducting magnet.

(b) RCA-NASA 13.6-T Solenoid

Prior to the magnet described above, RCA had completed for NASA[10] another solenoid with a bore of 15 cm and a central field of 13.5 T. The axial bore length is approximately 34.5 cm (Fig. 11). The overall current

density of the entire magnet is 9.25×10^3 A/cm^2. However, the minimum current density achieved in the inner modules at 14 T is 1.1×10^4 A/cm^2, which was obtained by means of copper shorting strips across each layer used to stabilize the magnet. The magnet consists of 26 modules and has a field energy of 2 Mj. Unfortunately, due to the presence of the copper strips across each layer, the magnet charging time is affected severely and was more than 17 hours, which for many applications limits its usefulness.

(c) SLAC 7-T, 30-cm, Helmholtz magnet[11]

The SLAC magnet, completed in October 1967, has a bore diameter of ~ 30 cm and a working bore of 20 cm for room temperature access. It comprises six separate modules, each self-supporting. To current optimize the magnet, each module is energized from separate current-regulated power supplies. Figure 12 illustrates overall dimensions, as well as the conductor configuration. The composite cable, a predecessor of the above-mentioned multistrand composite, is based on Nb(22 at %)Ti wires and copper filaments roped together and spirally wrapped with a nylon braid as interturn and interlayer insulation, and to provide adequate coolant passages. Based on heat transfer measurements by Wilson[12] and Whetstone,[6] an initial gap of 0.5 mm between turns was chosen for the passage of liquid helium, yielding a maximum surface heat flux value of 0.4 W/cm^2 in case of flux disturbances, while the stable operational current of 500 A in the magnet corresponds to a heat flux value of 0.360 W/cm^2 on the conductor surface, generating in the bore a field of 7 T. The average current density in the magnet is 4000 A/cm^2. However, after repeated operations and quenches, it is doubtful that the coolant gaps have retained their original shapes.

The indication of several short circuits in each module substantiates the assumption that the insulation has fatigued and is ruptured in a few areas, affecting primarily the charging time of the magnet which is about two hours. This insulation scheme, used already in several magnets, has disadvantages. The nylon embrittles at low temperatures and fatigues and ruptures under severe magnetomechanical stress. Unfortunately, all attempts to insulate high-resistance metallic strips with suitable thermosets had failed, necessitating the use of the organic multistranded tapes.

The magnet has a total weight of 1600 kg and 42,000 meters of cable were wound in the coil. It operates in a closed loop refrigeration system. When fully energized to 7 T, the helium boil-off is about 16 liters/hour, and at 6 T, about 9 liters/hour. The magnet is directly cooled down with gaseous helium from a 7-W liquefier to 20° K. To cool down the magnet to 4.2° K and to fill the magnet dewar, about 500 liters of helium are required. The central coil section (II) consists of a single .076-cm diameter Nb(22 at %)Ti conductor, exhibits training, and is fluxjump-sensitive. The magnet modules are permanently connected to low-inductance water resistors and to current-regulated power supplies through fast-acting switches (Fig. 13 and 14). When the breaker is activated, more than 80% of the energy is dissipated within 200 milliseconds into the resistance. Thus only a fraction of the helium, in which the magnet is immersed, is evaporated.

Double helical gas-cooled leads with a loss factor of 1 mW/A/lead to 1.5 mW/A/lead at a 1000-ampere current level are utilized to energize separate modules. It is planned to energize the magnet from external power supplies and then regulate the field by means of fluxjumps (10 watts) and disconnect the leads from the current source.

(d) The LRL light-weight, 1-m-diameter, 1-T magnet[13]

This magnet, part of an exciting experimental setup, is used for cosmic-ray experiments in a high-energy range of 300 GeV or higher. As the mean free path for such high-energy particles in the atmosphere is 50 g/cm^2 and the surface mass on the earth's atmosphere is 10^3/g cm^2, the experiment must be carried out at high altitudes. The experimental setup (Fig. 15) must be carried by means of a balloon and, in addition to the magnet, it consists of a momentum analyzer for primary radiation, a hydrogen target, and a second momentum analyzer for radiation products.

The main features of the magnet are light weight, a transverse field of 1 T over a cylindrical bore of 1-m diameter, large aperture to capture a reasonable number of events during a 24-hour flight, small heat leak and helium evaporation (< 5 liters/hour) so the balloon need not carry too much helium; it must be mechanically rigid to withstand shocks when landing (aluminum support frame), and it must operate in a persistent mode. The coil can be quenched by remote control, if necessary.

The coil is wound with a 19-strand composite cable, including three strands of 0.057-cm NbTi filament (Fig. 16). A central field of 0.85 T was measured at an operational current of 800 A. The magnet field energy is approximately 10^6 joules. The total weight of the magnet and dewar system is 2000 kg. The field at the conductor is calculated to be 2 T. The coil overall current density is 18,000 A/cm^2, and the coil field decay time constant is 8.6 seconds.

(e) BNL magnet for measuring magnetic moments of Ξ^-[14]

K^-, passing through a hydrogen target, decays into K^+ and Ξ_1^-. Ξ_1^- and K^+ decay further inside a tapered high field of 12.5 T into a Λ^0 and π^-.

Λ^0 decays further into a p and π^-. A spark chamber is located directly at the open end of the magnet; cylindrical spark chambers and Cerenkov counters surround the target.

The amount of precession due to the magnetic field can be calculated from the decay products. Since the rotation is equal to the magnetic moment of the particle, multiplied by the total field distance integral, the magnetic moment is established if the magnetic field is known precisely. In order to get good resolution at the expected value of the magnetic moment, a field distance product of 10^6 G/cm is required over the particle's flight path. Since the lifetime of the π^- is very short (average travel distance is approximately 10 cm), the average magnetic field must be 10 T.

The magnet is layer-wound with 2.25 mm vapor-deposited Nb_3Sn tape, has an inner tapered bore diameter of 3.8 - 6.6 cm with a half-angle of 8° equal to the production angle of Ξ^-, and generates over 10 T at the 3.8-cm bore end. It is assumed that with some modifications, the maximum field can be boosted up to 12.5 T.

Manufacturing limitations prevented production of the Nb_3Sn ribbon in long lengths and thus the magnet is constructed of 14 separate tapes. Each tape has different amounts of Nb_3Sn deposited on Hastelloy in order to obtain optimum performance of the coils as a function of field. Tapes with the highest current at highest field are used at the 3.8-cm bore end. The magnet consists of four concentric, physically separable modules or sections (Fig. 17).

The coil forms are constructed of perforated stainless steel and coated with Teflon for insulation. The inner two sections have anodized aluminum

foil as layer-to-layer insulation, while the outer two sections have mylar-copper-mylar sandwich layer insulation. Copper shorting strips are placed across each layer to prevent voltage buildup and arcing, should the coil go normal.

The magnet is supplied with helium continuously from a 3-watt helium liquefier. Automatic sensing devices keep the helium level in the magnet dewar nearly constant. Closed loop refrigeration cycle is utilized.

(f) Polarized proton target magnet, Saclay[15]

The magnet is part of the experimental setup for the CERN Proton Synchrotron for use in a π-p scattering experiment with a polarized target. Protons are polarized in the reaction plane parallel or perpendicular to that of the incident π, enabling measurements of the A and R parameters. The magnet shown in Fig. 17 has a central field of 2.5 T and a field homogeneity of 10^{-4} over a 5-cm diameter sphere. The field axis is horizontal; a vertical access is foreseen for the target dewar penetration. The magnet entrance and exit of the beam are 90° tapered for beam entry. The conductor, a 19-strand cable, consists of six 0.25-mm diameter Nb(25%)-Zr wires, copper-coated and heat-treated, and 13 copper strands of 0.35-mm diameter. Open structure has been adapted for penetration of coolant and every turn is insulated by means of a nylon yarn. Concentric layers are separated by means of a nylon screen. Maximum current level attained is 285 A, corresponding to a field of 2.5 T in the center of the magnet and 4 T at the conductor. The magnetic field energy in the magnet is 400 kj.

The magnet coil consists of four concentric modules; approximately 28,000 meters of conductor were wound in the coil. Each section is wound on a

copper form, producing a short-circuited on-turn secondary winding inductively coupled to the main windings to protect the magnet, if the coil should go normal. Overall current density in the magnet is reported to be 15,000 A/cm^2!

The charge-up speed of the magnet between 0.5 T and 2.5 T is slow and varies between 5 and 2 gauss/second. The magnet analogue to the SLAC magnet is charged in a time of two hours, indicating short circuits between turns and layers.

The list can be continued by describing the MHD magnet built by Avco,[16] with an i.d. of 30.5 cm and maximum field of 3.6 T, with an energy of 3.6 Mj; the Helmholtz magnet by CERN[17] with an i.d. of 40 cm and a central field of 6 T; the Helmholtz magnet by ANL[18] with a bore of 28 cm and a field of 4.5 T; and the Helmholtz magnet by BNL[19] with a bore of 20 cm and a stable field of 3.7 T, partially stable field of 5.1 T; the minimum field magnet for plasma confinement with a spherical inner space of 25 cm and an approximate 3.8-T field at the conductor built by LRL-Livermore[20]; several 10-T magnets combined with fluxpumps to energize the magnet built by GE,[21] etc., but for space reasons, detailed description is omitted.

IV. BEAM TRANSPORT MAGNETS

Superconducting beam transport magnets are of interest in high-energy applications mainly because of the high-field characteristics of superconductors type II. While generally in room-temperature, water-cooled, magnets, the field at the pole tips seldom exceeds values of 2 T, superconducting magnets are currently being built or have been tested, with fields at the conductor in excess of 4 T and quadrupoles with field gradients up to 0.7 T/cm.

Iron, which is predominantly responsible for the magnetic field shape and distribution in water-cooled magnets plays the secondary role of shielding the fringing field from the environment, contributing some additional field of about 0.8 - 1.2 T to the field generated by the coils, and as structural material to support coils, dewars, and vacuum tanks in superconducting magnets. The field distribution is primarily dictated by the MMF or current density distribution in the coils. Coil end effects become more predominant and thus new designs and design criteria were developed in order to achieve good field or gradient homogeneity over the effective length of the magnet. Correcting coils become necessary. A first- and second-order optical treatment of this new generation of magnets is still lacking but is currently being studied at various places.

To generate a p-pole field, many solutions are currently being investigated, such as dipole fields generated by coils having a cross section of intersecting circles or ellipses,[22] current distribution as parts of a cylinder, square or rectangular blocks, etc. But basically the current or current density must be distributed over the perimeter of the cylindrical bore according to

$$i = i_0 \cdot \cos\left(\frac{p}{2}\,\theta\right) \tag{1}$$

For a coil having the inner and outer radii a_1 and a_2, respectively, (Fig. 18), the magnetic vector potential is derived to be:

$$A_z(r,\theta) = \frac{\mu_0 i_0}{p} \cdot r^{p/2} \cos\left(\frac{p}{2}\,\theta\right) \int_{a_1}^{a_2} \frac{dR}{R^{\frac{p}{2}-1}} \tag{2}$$

which gives for a dipole configuration with p = 2:

$$A_z(r,\theta) = \frac{\mu_0 i_0 r}{2} (a_2 - a_1) \cos\theta \ , \tag{3}$$

a quadrupole configuration

$$A_z(r,\theta) = \frac{\mu_0 i_0 r^2}{4} \ln\left(\frac{a_2}{a_1}\right) \cdot \cos(2\theta) \tag{4}$$

For p = 6, 8 . . . (sextupole, octupole, etc.), we have:

$$A_z(r, \theta) = \frac{2\mu_0 i r^{\frac{p}{2}} \cos\left[(p/2)\theta\right]}{p(p-4)} \left[\frac{1}{a_1^{\frac{p}{2}-2}} - \frac{1}{a_2^{\frac{p}{2}-2}} \right] \qquad (5)$$

If the current-carrying conductors are arranged over the surface of a cylinder, parallel to its axis and so distributed that the current density around the cylinder is proportional to cos θ (for dipoles) and cos 2θ (for quadrupoles), a perfect dipole or quadrupole field is produced over the median plane.

Good quadrupole or dipole fields can be generated when conductors carrying co constant current density are distributed over the cylinder perimeter in steps approximating cos θ distribution,[23] according to Fig. 19. Various bending and quadrupole magnets have been already constructed by BNL. Among others, Fig. 20 illustrates a bending magnet and Fig. 21, a quadrupole magnet, built with Nb_3Sn ribbon, carrying constant current. The steps are produced by placing the conductors in slots distributed according to cos 2θ law. The quadrupole has an aperture diameter of 10 cm and a length of 60 cm, with a field gradient of $\sim$ 7 kG/cm. The construction of single-layer bending and quadrupoles is simple, using Nb_3Sn tapes and edge-cooling. However, if several current-carrying layers become necessary to produce a specified field or gradient, the coil geometry becomes more complicated and field-shaping more cumbersome. Thus, for this design, high current density coils become imperative, to eliminate additional layers.

A dipole magnet using Nb_xTi is currently being built at RHEL.[24] As shown in Fig. 22, the uniform field over the median plane is produced by a current distribution of approximately elliptical shape. The magnet has an effective length of 1.4 m (total overall length, 2 m) and a room-temperature aperture

of 17 cm. With an overall current density in the coil of 7200 A/cm^2, the magnetic field in the center is 4 T. 350 kg of stabilized Nb(60%)Ti conductor (0.38-cm diameter) is wound to a shape illustrated in Fig. 23. The total lateral force on the conductor is 3100 kg and the expected boil-off rate for helium is 2 - 4 liters per hour.

Other beam transport magnets are the 1-m long, 15-m aperture, dipole coil with a transverse field of 2 - 2.5 T at ANL,[25] and the CERN-Culham joint project quadrupole.[26]

In all new beam transport magnets, it is expected that at transverse fields of 5 T at the conductor, current densities of 5×10^4 or higher must be achievable.

To cancel external fringing fields, the dipole or multipole may be surrounded by another dipole or multipole coil of larger aperture, which cancels the external field. However, it seems more economical to build iron-bound magnets (laminated yokes for ac application), which shield the fringing field. The iron is at room temperature. However, non-uniform saturation in the iron may affect adversely the field homogeneity or distribution inside the aperture. Unfortunately, operational experiences with beam transport magnets in combination with high-energy beams are presently non-existent. Also data on irradiation effects are scarce.[27] For some applications, it may be advisable to leave the median plane free of current-carrying conductor, so that, in case of beam missteering, charged particles would not collide with the conductor material. The generated heat may destroy the inter-turn insulation and, due to generation of short circuits, may lead to sudden changes of the coil inductance and possible fluxjumps which may quench the coil.

V. EXPERIMENTAL MAGNETS

Several large bubble-chamber magnets have been constructed or proposed in the recent two to three years. A survey of these magnets, approximate energy and cost, is given in Fig. 24. As mentioned, emphasis on high current density and compact design is shifted towards reliable magnets where the conductors are not stressed beyond their elastic limit and, in case of a quench, the coil is protected internally by means of ample normal metal such that if the field energy is converted to Joule heating, the conductor temperatures should not exceed certain predetermined values.

Magnets are completely stabilized by means of copper or aluminum substrates, where the copper-to-superconductor ratio exceeds 5:1 and the filament diameter does not follow necessarily the intrinsic stabilization requirement, limiting the maximum current through each filament below its critical value.

Rectangular or square-shaped conductors are now commercially available for transport current exceeding 5000 A in continuous lengths of 200 m or more. The number of filaments in these conductors varies between 6 and 500, with filament sizes varying between several mm to hundreds of mm in diameter. Most magnets are composed of double pancakes with axial and radial spacers for the coolant passage, one- or both-sided radial reinforcements combined with appropriate insulation tapes.

Some attempts to utilize hollow composite conductors and eliminate the helium container are being made at BNL,[28] CERN,[29] and SLAC.[30]

In these magnets, internal joint problems are an important factor. Electron beam welding, explosive methods, or overlapping and flaring of the conductor have been utilized.

The main concern shifts towards magneto-mechanical stresses on the conductor. Although the superconducting filament based on Nb_xTi has a yield strength

of $\sim 9 \times 10^3$ kg/cm^2, and the copper a yield strength of $\sim$ 800 kg/cm^2 at 4.2° K, it is advisable not to strain the composite conductor beyond its 0.1% yield strength. Strain on the conductor must be kept within the elastic limit of the composite to prevent conductor elongation, which may result after a few magnet operations in a loosely-wound coil. A loosely-wound coil becomes fluxjump-sensitive due to macroscopic wire movements. Work hardening due to conductor strain influences coil stability.

Prestressing the conductor during winding is an important parameter, in order to avoid any minor conductor movements. Current densities over the composite conductors are kept around 10^4 A/cm^2 at 7-T fields, which yield tangential stresses on layer-wound coils of around 2.5×10^3 kg/cm^2, which is beyond the yield strength of annealed copper at 4.2° K. Reinforcing strips become necessary.

Reinforcement tapes wound bifilar with the conductor incorporate appropriate coolant passages as well, thus elaborate schemes have been developed by several laboratories. I briefly summarize the achievements to date from several magnets being built or currently tested, in chronological order:

(a) The ANL Bubble-Chamber Magnet[31] (Fig. 25)

The magnet, an iron-bound structure, has a central field of 2 T and a diameter of 3.7 m. The conductor, a rather conservative design (5 cm × 0.254 cm), carries 2000 amperes and thus the overall current density in the conductor is 1.574×10^3 A/cm^2. Six superconductors are imbedded in the copper matrix. The field energy of the magnet is $\sim$ 150 Mj. Hoop stresses on the conductor are 45 kg/cm^2. Thus no reinforcements were necessary. The weight of the copper used in the coil is 45,000 kg and of the superconductor, 300 - 450 kg. ANL started to cool down the magnet by the end of September 1968 by means of liquid N_2 and liquid H_2, and has kept it since at 100° K to be ready when the refrigerator is installed.

(b) The BNL 2.4-m Bubble-Chamber Magnet[32] (Fig. 26, 27)

This magnet was completed in July 1968 and cooled down to about 7° K at that time. The magnet was partially energized. Test was interrupted further in order to modify and improve the cooling scheme.

The next operation will be in combination with the bubble-chamber assembly for the forthcoming neutrino experiment in December 1968. Basically the same considerations of the conductor shape and cooling scheme will prevail as for the ANL Bubble Chamber. However, due to higher stresses on the conductor, the conductor is reinforced by means of a stainless steel tape. The coil is wound in pancake arrangement. The composite conductor has a cross section of (5.08×0.2) cm^2 and carries a stable current of 6000 amperes ($J_{cond} = 5320$ A/cm^2). The central magnetic field is 3 T with a field at the conductor of 4 T. Approximately 75% of the conductor outer surface is cooled by means of helium. An elaborate reinforcing and cooling structure is incorporated in the coil. The chosen heat flux of 0.33 W/cm^2 during operation is dictated rather by hoop stresses of 640 kg/cm^2 than the coil design and cooling scheme. The magnet has no iron return path; its inner diameter is 2.4 m; the weight of the conductor is about 15,000 kg. Its total field energy is $\sim$ 60 Mj.

(c) The CERN 4.7-m, 3.5-T, Bubble-Chamber Magnet[33] (Fig. 28)

When completed in 1970, this will be the largest magnet in the world. It is in a Helmholtz configuration, as are the two previous bubble-chamber magnets, and the conductor $(6.1 \times 0.3$ cm) carries a current of 5700 A. The weight of the copper used in the conductor is 96,000 kg, and the weight of the Nb_xTi, 3000 kg. The magnet is equipped with a room temperature return yoke, primarily to balance the forces and reduce fringing fields around the magnet. The magnet field energy is 780 Mj!

Two other bubble-chamber magnets, currently in the proposal stage, are the Rutherford 7-T, 1.9-m diameter, bubble-chamber magnet,[34] and the SLAC 1.5-m, 7-T, Helmholtz magnet.[35] The latter is intended as a conversion of the existing 2.6-T water-cooled magnet and has a horizontal axis, while all other magnets described above have vertical axes. Cooling problems in the SLAC magnet are more complicated and, due to space restrictions (the existing iron return path is being utilized), support more difficult. The SLAC magnet will have a stored energy of $\sim$ 100 Mj and a conductor current density of $\sim$ 5000 A/cm^2.

VI. ACCELERATOR MAGNETS

In the case of dc accelerators, major magnet problems are the same as already mentioned. However, superconductivity opens new vistas in the area of slow-cycling ac accelerator magnets. Superconductors type II are lossy, if operated beyond H_{c_1}, fluxjump and fluxcreep resistivities are encountered, which are given, according to Wipf,[36] for semi-infinite cylindrical wires as:

$$\rho_{creep} = 2.5 \times 10^{-9} \frac{r_0}{J_c} \cdot \frac{\partial B}{\partial t} \tag{6}$$

and

$$\rho_{jump} = 1.5 \times 10^{-10} \frac{\partial B}{\partial t} \tag{7}$$

Loss per cycle per unit surface can be given, according to Bean,[37]

$$P = \frac{10^{-6}}{12(\pi)^2} \cdot \frac{\Delta B^3}{J_c} \left(\frac{\text{joule}}{\text{cm}^2}\right) \tag{8}$$

and is independent of frequency, provided that frequency is not raised to the point where eddy currents in the substrate or stabilizing matrix become appreciable.

However, as mentioned above, and predicted by Hancox,[38] J. P. Smith[39] and others, fluxjumps can be eliminated when the diameter of the superconducting filament is below a critical value given in Eq. (9). No fluxjumps in the conductor are encountered, if the following relations are met:

The average current density in the filament must be according to the relation

$$J_{av} = \frac{1}{d_n}\left[\frac{3\times10^9}{4\pi} C_p\delta \cdot \frac{d_s}{d_n} \cdot T_0\right]^{1/2} \tag{9}$$

and filament diameter to

$$d_f \leqq \frac{1}{J_c}\left(\frac{3\times10^9}{4\pi} C_p\delta \cdot T_0\right)^{1/2} \tag{10}$$

where

T_0 = $-J_c \cdot \frac{dT}{dJ_c}$ in °K

C_p = heat capacity, W/g°K

δ = density in g/cm^3

d_n, d_s = diameter of normal and superconducting conductor, respectively, in cm

This implies that wire diameters for Nb_xTi should be in the order of 5×10^{-3} cm to prevent fluxjumps. Wires in this form are commercially available. Another effect, which has been known for some time in electrical machines, has been found also for composite conductors: If the conductor length is greater than a critical value given in Eq. (11), magnetization currents flowing through superconducting filaments in opposite directions induce a voltage between these filaments. This voltage drives eddy currents through the normal metal and generates ac losses.

$$\ell_{crit}^2 = 10^8 \lambda J_c d_s \cdot \rho_n \frac{1}{\partial B/\partial t} \qquad (11)$$

with λ being the space factor.

If the magnetic field is charged at a rate of 6 T/sec, the critical length is only a few mm long. The induced voltage in the substrate can be reduced by:

(a) Twisting or transposition of the superconductors, such that the pitch of the twist is smaller than ℓ_c.

(b) Increase in ρ_n in the substrate, by using alloys such as cupro-nickel proposed by Smith,[39] or make the substrate porous and nonconductive, as proposed by Brechna and Garwin.[5] In the latter case, twisting the conductor would be unnecessary. This proposal also has the advantage of better enthalpy stabilization due to the proximity of supercritical helium around the superconductor, which allows d_s to be increased. (See Eq. 10).

(c) Special treatment of the superconductor, such that dJ/dH over the field range where the magnet is operated is either zero or negative.

It becomes clear that accelerators will be based on separate function magnets, such as dipole and quadrupole magnets, with sporadic higher pole-correcting magnets (sextupoles). Fringing field corrections have to be performed by means of correcting dipole and quadrupole coils. Appropriate iron shielding at room temperature is recommended.

Problems such as fast magnet replacement in case of a damage, energizing and cooling magnets by means of centrally or separately located power supplies and refrigerators, the use of fluxpumps with magnets, are being studied.

In accelerator magnets, high current density in the active coil area is essential, and should be attempted in the 50,000 A/cm^2 range which, due to Lorentz forces, at coil ends, will automatically limit the maximum field at the conductor to 5 or 6 T. Magnet apertures in the order of 5 - 7 cm diameter should not, if possible, be exceeded.

VII. SPECIAL-PURPOSE MAGNETS

Among a whole array of different magnets for a variety of purposes, such as plasma experiments (levitated ring), NMR high-homogeneity magnets, magnets for the Ω project, I have selected two magnets, which are briefly described.

(a) Muon Storage Ring[40] (Fig. 29)

Preliminary studies subsequent to the 5-m CERN muon storage ring indicated that the next stage in building a muon storage ring would be either a room-temperature 10-m diameter magnet with a muon storage area of (10×15) cm^2 and a transverse field of 1.4 T, or a 5-m superconducting magnet with a transverse field of 5 T and a storage area of (6×8) cm^2. The storage ring for the third phase of the G-2 experiments, if the superconducting version is selected, has an energy of 40 Mj and its unique configuration, consisting of four concentric superconducting coils, makes the use of a hollow composite superconductor quite attractive. (Fig. 30)

The field over the storage area has weak focusing property with $n = 0.16$, tolerable index deviations shall not exceed $\frac{\Delta n}{n} = \pm 0.1\%$, in order to avoid fourth-order resonances. To comply with this requirement, the magnet consists of two parts:

(1) A dipole field coil with a field homogeneity of $\frac{\Delta B}{B} = 10^{-4}$ over the median plane, and a maximum strength of 5 T.

(2) Separate quadrupole coil to produce weak focusing with $n = 0.16$.

Azimuthal field homogeneity over the entire storage ring circumference should be 10^{-5}. Field distortion due to magnet cooldown or Lorentz forces will be corrected by means of auxiliary superconducting coils. Field reproducibility between successive runs must be $\leq 10^{-5}$.

The magnet is provided with iron shielding (room temperature) in order to shield measuring equipment and photomultipliers from the fringing field effect, and also to prevent field distortion is ferromagnetic parts are moved inside the laboratory surrounding the magnet. Conductor movements are restricted to less than 3×10^{-4} cm to prevent field distortion by impregnating the coil in rigid thermosets and by mechanical support structures.

Field measurement is performed by means of a Fermi trolley, combined with optical monitoring systems, such that a field at any point in the storage area can be recorded within one second. The magnet is energized by 7250 amperes. Coil weight is 16,000 kg, overall magnet current densities are $\sim$ 8000 A/cm^2 maximum.

The mode of experiment is by colliding the proton beam from the CERN Proton Synchrotron to an external target, producing π^-, which are guided through a superconducting tube to the storage area, where they decay into muons. μ^- will be stored for at least one rotation, prior to decay into electrons.

(b) Hybrid Magnet, MIT-NML[41] (Fig. 31)

A magnet where part of the field is generated by a nonsuperconducting (water-cooled), and the other part by a superconducting, coil. These magnets have the advantage that they can produce fields economically which cannot be produced by either part alone. The low field section (outer coil) is generated by a Nb_xTi composite conductor and the high field part (two inner coils) by a room-temperature magnet. The outer superconducting magnet generates a field of 6 T and has an inner diameter of $\sim$ 40 cm. The two inner coils, water-cooled copper discs (Bitter),

produce a field of 10 T and 7.5 T, respectively, over a bore of 3.8 cm. The magnet can be charged to the full field of 23.5 T in 20 minutes. The total power absorption due to the room temperature magnets would be about 6.5 MW.

Hybrid magnets may be useful in many laboratories where high fields are required, while no high power and appropriate water-cooling are available.

VIII. SUMMARY AND CONCLUSIONS

The above descriptions of the most important magnets, available or currently being built, illustrate the advances of the past two to three years in superconducting magnets. High-energy magnets can be built as reliably and as economically as room-temperature magnets. Magnetic fields produced even by complicated coil configurations can be predicted precisely, and magnets can operate reliably.

There are, of course, areas where considerable work lies ahead, such as study of the performance of magnets in combination with high-energy beams, refrigerators, power-supply systems, fluxpumps. Energy dissipation from large accelerators must be studied. Material behavior, insulation degradation fatigue properties, irradiation damage in superconducting and nonsuperconducting parts, must be considered in detail. But it can be seen from the above that superconducting magnets have found their important place in many areas of physics.

ACKNOWLEDGMENTS

The author is indebted to many colleagues in various laboratories, specifically to D. B. Montgomery (NML), A. Prodell (BNL), J. Purcell (ANL), S. St. Lorant (SLAC), P. F. Smith (RHEL), C. Taylor (LRL), M. N. Wilson (RHEL), and F. Wittgenstein (CERN), for providing figures, data and measurements, which have been incorporated into this paper.

REFERENCES

1. P. S. Swartz and C. P. Bean: Bull. Am. Phys. Soc. 10, 359 (1965).
2. S. L. Wipf: Phys. Rev. 161, No. 2, 404 (1967).
3. H. Brechna: SLAC-PUB-464 (1968).
4. R. Hancox: Proc. Intermag Conf., Washington, D. C. (1968).
5. H. Brechna and E. L. Garwin: SLAC Proposal (1967).
6. C. W. Whetstone and R. W. Boom: Paper B6, Advances in Cryogenic Engineering, Vol. 13, p. 68 (1968).
7. A. C. Prior: Cryogenics 7, No. 3, 131 (June 1967).
8. S. St. Lorant: Private communication.
9. H. C. Schindler: Applied Superconductivity Conference, Gatlinburg, Tennessee (1968).
10. E. R. Schrader and P. A. Thompson: RCA Report (1967).
11. H. Brechna, et al: SLAC-PUB-337 (1967).
12. M. N. Wilson: RHEL Paper II-2, IIR Commission 1 Meeting (1966).
13. Clyde E. Taylor, et al: UCRL-70285, Rev. 1 (1967).
14. W. B. Sampson: Proc. Intl. Conf. Magnet Technology, 530 (1965).
15. H. Desportes and B. Tsai: Proc. Intl. Conf. Magnet Technology, 509 (1965).
16. Z. J. J. Stekly, et al: AVCO E.R.L. AMP 210 (1966).
17. F. Wittgenstein: Private communication.
18. C. Laverick and G. Lobell: Rev. Sci. Instr. 36, No. 6, p. 825 (1965).
19. J. A. Bamberger, et al: Paper C4, Advances in Cryogenic Engineering, Vol. 13, p. 132 (1968).
20. Clyde E. Taylor and C. Laverick: Proc. Intl. Conf. Magnet Technology, 594 (1965).
21. C. H. Rosner, M. G. Benz and H. R. Hart, Jr.: G.E. Publications (1966-1968).

22. A. Asner, et al: Proc. the Second Intl. Conf. on Magnet Technology, 32 (1967).

23. W. B. Sampson: Proc. the Second Intl. Conf. on Magnet Technology, 574 (1967).

24. M. N. Wilson and J. D. Lawson: Summer Study on Superconducting Devices and Accelerators, BNL (1968).

25. J. Purcell: Private communication.

26. D. N. Cornish and A. Asner: Summer Study on Superconducting Devices and Accelerators, BNL (1968).

27. H. Brechna: SLAC-PUB-469 (1968).

28. A. Prodell: BNL Proposal, 25-foot Bubble Chamber (1968).

29. M. Morpurgo: CERN NP Int. Rep. 67-15 (1967).

30. H. Brechna: ANL Rep. 7192, 29 (1966).

31. J. Purcell: Applied Superconductivity Conference, Gatlinburg, Tennessee (1968).

32. A. Prodell: Applied Superconductivity Conference, Gatlinburg, Tennessee (1968).

33. CERN Study Report: TC/BEBC 66-73 (1966).

34. Rutherford Design Study, RL/S/100 (1967).

35. SLAC Design Study: Proposal II (1968).

36. M. S. Lubell and S. L. Wipf: J. Appl. Phys. 37, 1012 (1966).

37. C. P. Bean: Rev. Mod. Phys. 36, 31 (1964).

38. R. Hancox: Phys. Letters 16, 208 (1965).

39. J. P. Smith, et al: Rutherford RPP/A 43 (1968).

40. H. Brechna, et al: Study of a Superconducting Muon Storage Ring, CERN (unpublished).

41. D. Bruce Montgomery, et al: Paper D1, Cryogenic Engineering Conference (1968).

Figure Captions

1. Stabilized Cable (AI)
    1. Copper conductor
    2. Superconductor
    3. Indium
2. Composite conductor (Cryomagnetics)
    1. Copper matrix
    2. Superconducting filament
3. Composite conductor (Airco)
    1. Copper matrix
    2. Superconductor
4. Nb_3Sn
    a. RCA
    b. General Electric
5. Conductor surface heat flux vs coolant gap in the helium nucleate boiling region (Whetstone).

   Unrestricted helium flow results in a maximum value of 0.78, while in most magnets, the heat flux measured is about 0.4 W/cm^2.
6. Conductor surface heat flux vs helium temperature (Whetstone).
7. Critical super current density vs applied transverse magnetic field

   dashed line: short sample

   solid line: small coil performance
8. Cost of superconductors vs applied magnetic field (Prior). The values are for simple conductor geometries. Data for composite conductors may be obtained directly from vendors.

9. Overall cost of refrigeration plants (no buildings) vs net refrigeration output (S. St. Lorant)
    1. Helium Refrigeration System
    2. Hydrogen Refrigeration System
10. Total installed power vs net refrigeration output (S. St. Lorant)
    1. Helium Refrigeration System
    2. Hydrogen Refrigeration System
    3. Nitrogen Refrigeration System
11. NASA 13.6-T, 15-cm bore, superconducting solenoid. The coil is current-optimized and consists of 26 modules.
12. SLAC 30-cm, 7-T, Helmholtz Magnet.
13. SLAC 30-cm, 7-T, Helmholtz Magnet. The magnet consists of six self-supporting current-optimized modules.
14. SLAC superconducting coil installation.
    1. Magnet dewar
    2. ADL Liquefier (7 W)
    3. High-voltage switch
    4. Water resistance
    5. Gas bag
    6. Liquid helium transfer line
    7. Helium gas exhaust line
15. LRL light-weight high-altitude experimental equipment.
16. LRL superconducting magnet for high-altitude experiments. The magnet has a one-meter diameter and a central field of ~ 1 T.
17. BNL magnet for measuring the magnetic moment of Ξ.

18. Polarized proton target magnet, Saclay.

19. Ampere-turn distribution and cross-sectional view of a BNL single-layer quadrupole.

20. BNL - 4" superconducting quadrupole .

21. BNL - superconducting bending magnet.

22. RHEL - superconducting bending magnet.

23. RHEL - superconducting bending magnet during winding.

24. Proposed and procured bubble-chamber magnets for high-energy physics (P. F. Smith).

25. The ANL, 3.7-m, 2-T, superconducting bubble-chamber magnet. The picture illustrates half of four-module Helmholtz configuration.

26. Cross-sectional view of the BNL 2.4-m superconducting bubble-chamber magnet.

27. BNL 2.4-m, 3-T, superconducting bubble-chamber magnet.

28. CERN 4.7-m, 3.5-T, superconducting bubble-chamber magnet.

29. Cross-sectional view of the proposed CERN muon superconducting storage ring.

    1. Hollow superconductor (see Fig. 30) for dipole coil.
    2. Quadrupole coil.
    3. Correcting coil.
    4. Iron return yoke.
    5. High-voltage loop.
    6. Magnetic field measuring device.
    7. High-pressure helium gas inlet.
    8. Low-pressure helium gas outlet.

30. Hollow superconductor (IMI)

    1. Supercritical helium passage.
    2. Superconducting filament.
    3. Copper matrix.

31. The MIT-NML hybrid magnet.

    1. Superconducting coil.
    2. Room temperature water-cooled coil
    3. Water-cooled Bitter discs

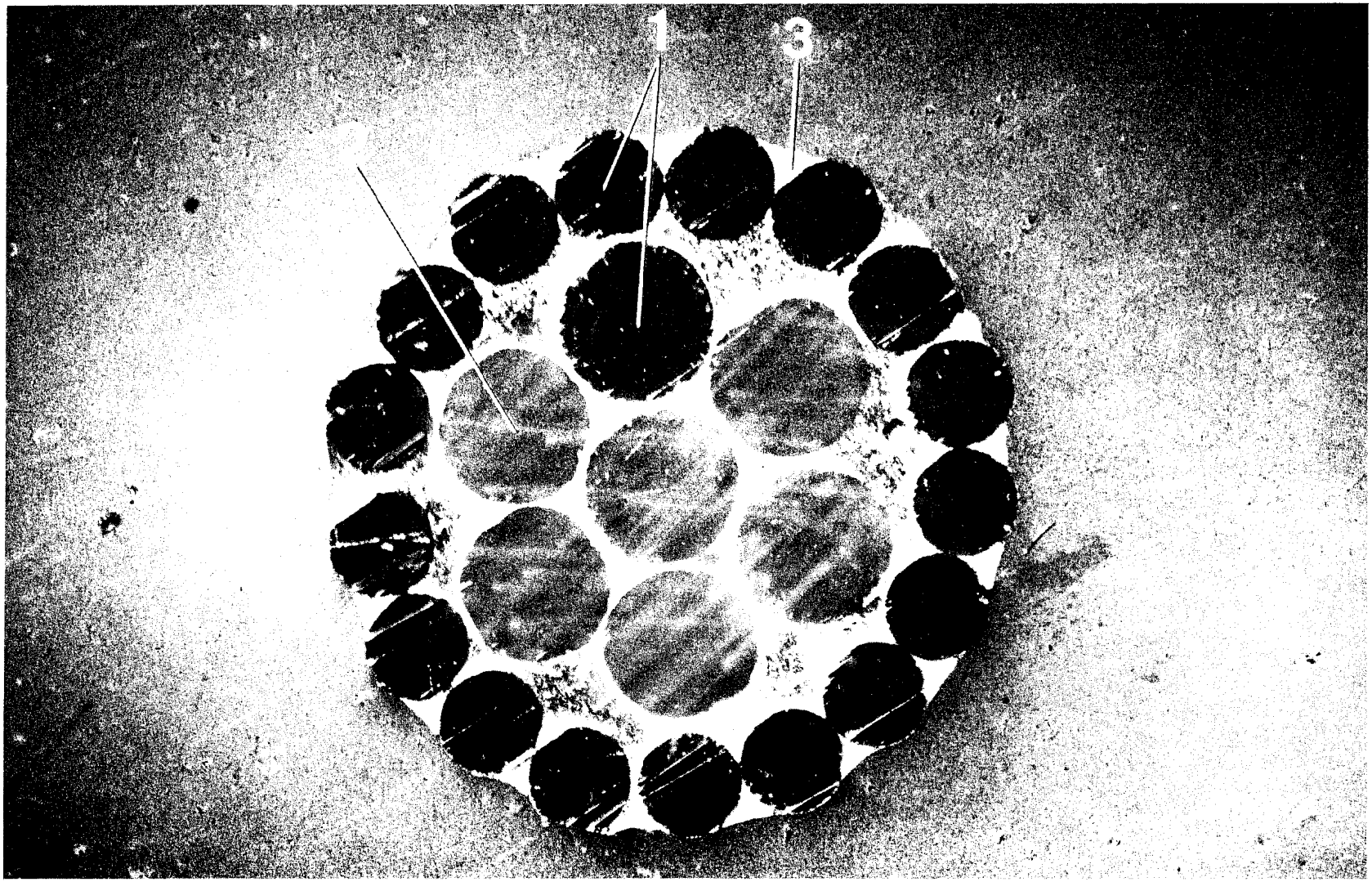

1050A25

Fig. 1

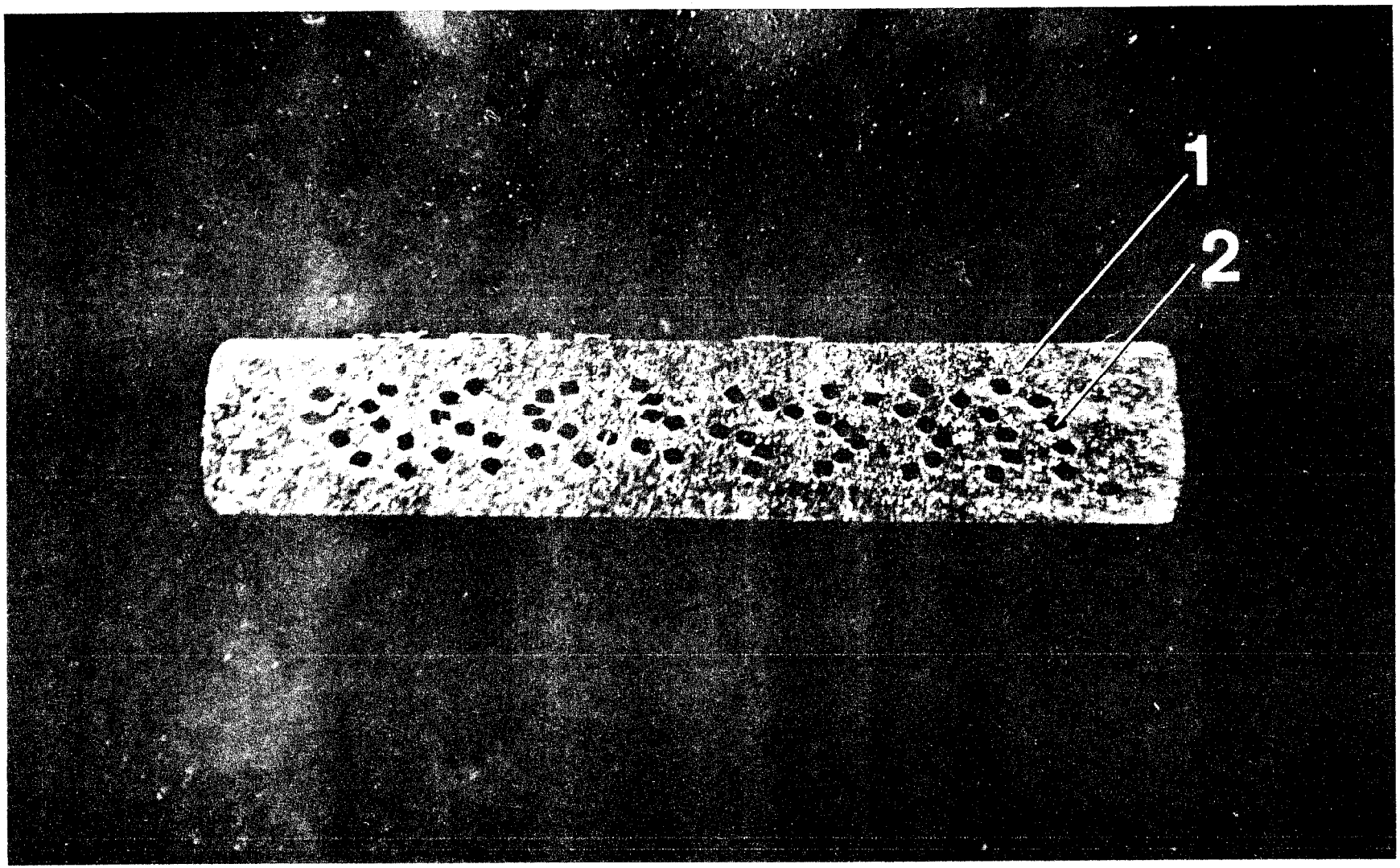

Fig. 2

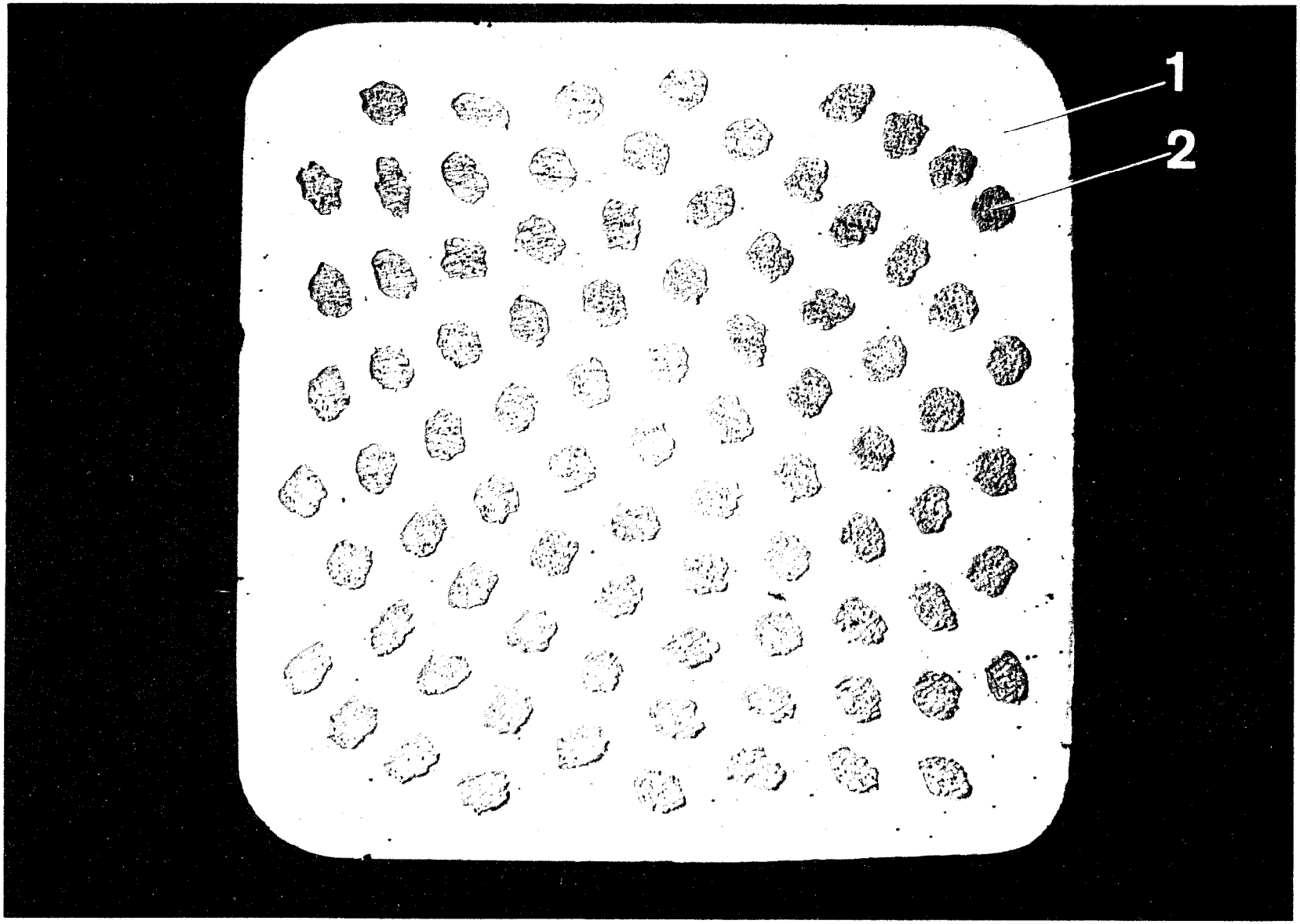

Fig. 3

1050423

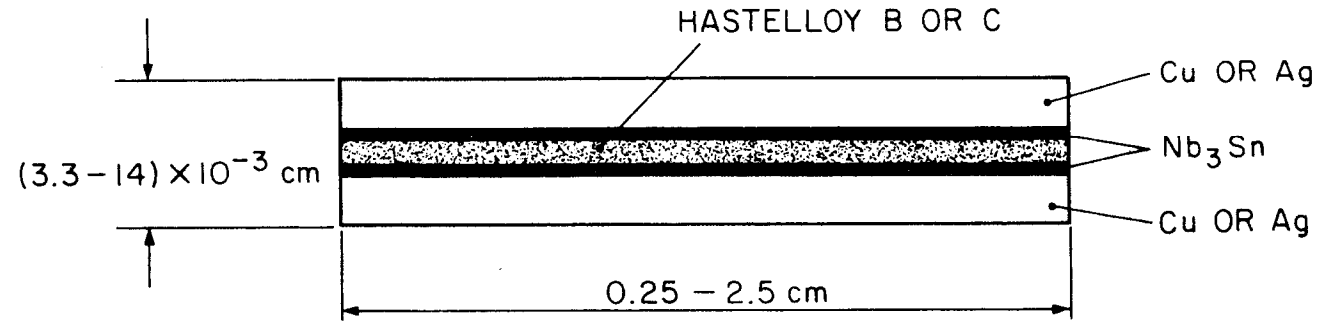

a.

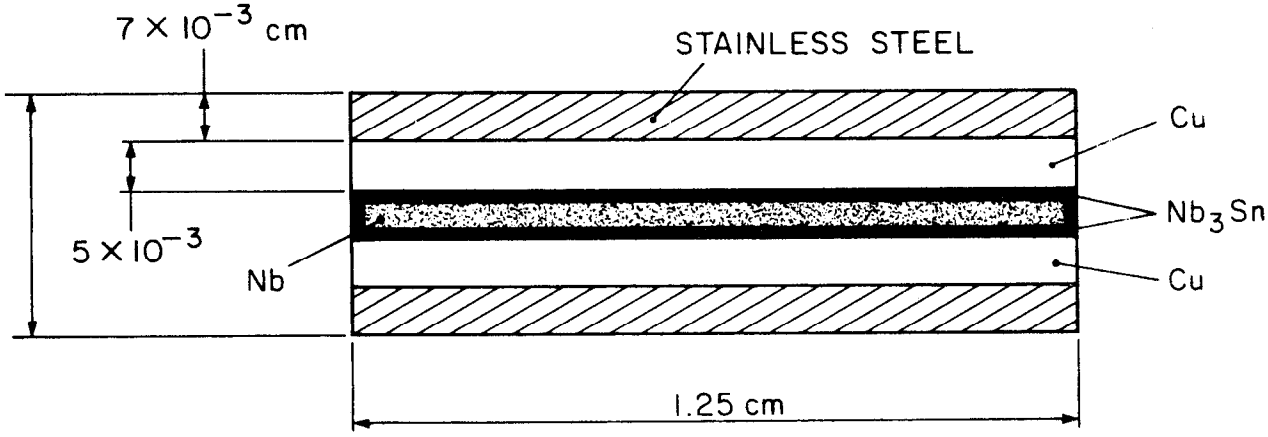

b.

1170A8

Fig. 4

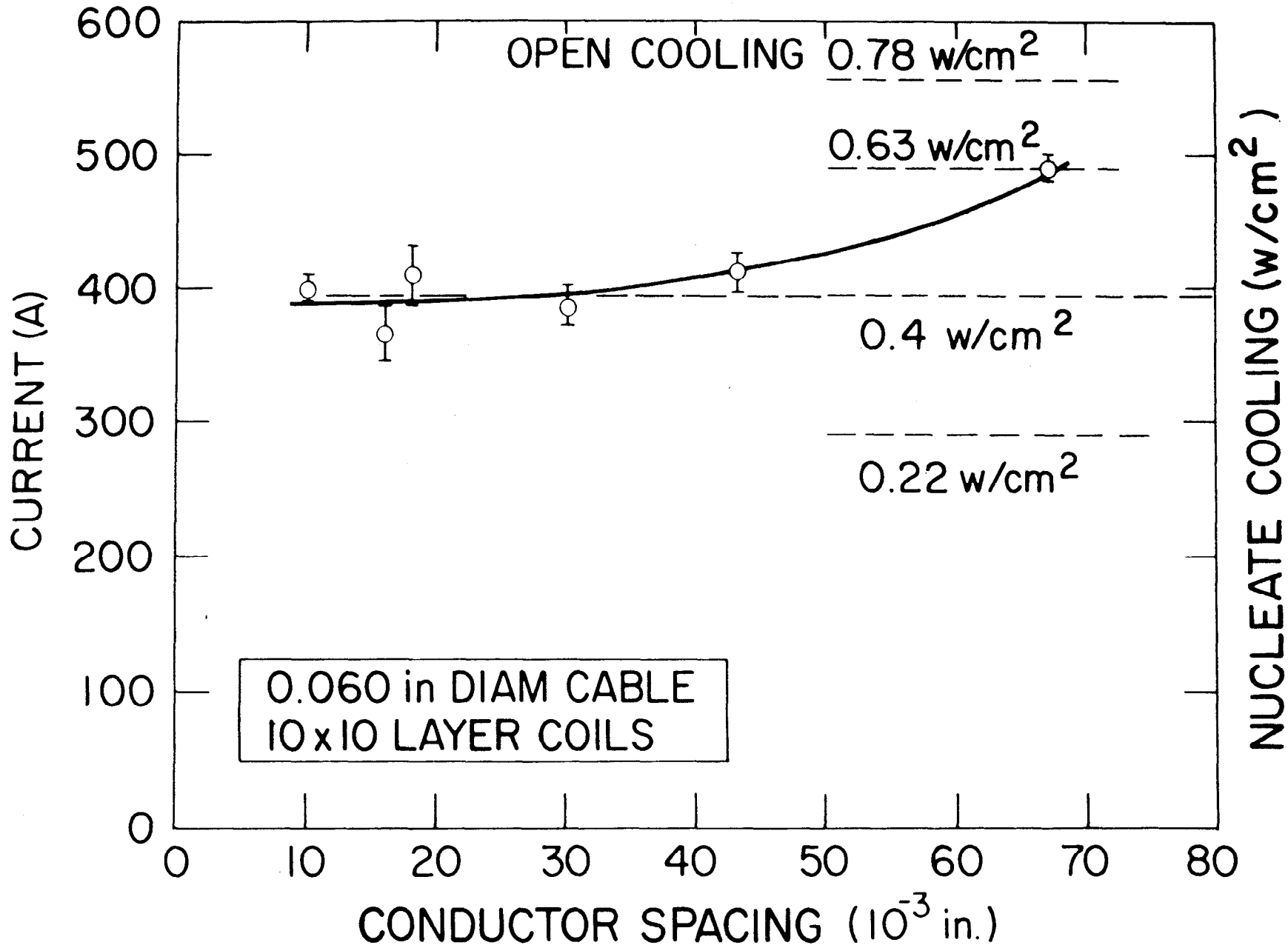
OPEN COOLING 0.78 w/cm2
0.63 w/cm2
0.4 w/cm2
0.22 w/cm2
0.060 in DIAM CABLE
10 x 10 LAYER COILS
CURRENT (A)
NUCLEATE COOLING (w/cm2)
CONDUCTOR SPACING (10-3 in.)
0
100
200
300
400
500
600
0
10
20
30
40
50
60
70
80

Fig. 5

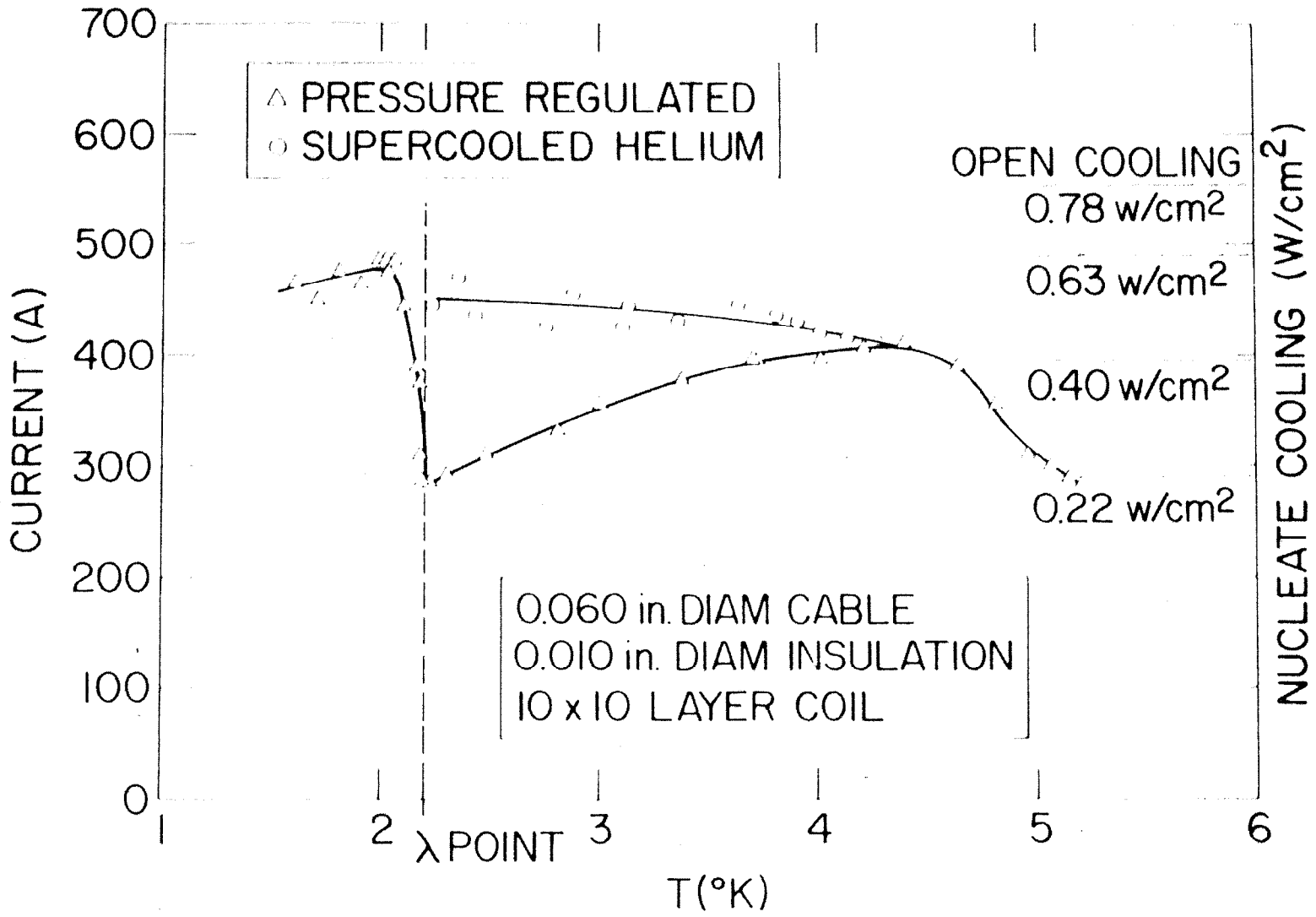
700
600
500
400
300
200
100
0
CURRENT (A)
PRESSURE REGULATED
SUPERCOOLED HELIUM
OPEN COOLING
0.78 w/cm2
0.63 w/cm2
0.40 w/cm2
0.22 w/cm2
0.060 in. DIAM CABLE
0.010 in. DIAM INSULATION
10 x 10 LAYER COIL
NUCLEATE COOLING (W/cm2)
2
λ POINT
3
4
5
6
T(°K)

Fig. 6

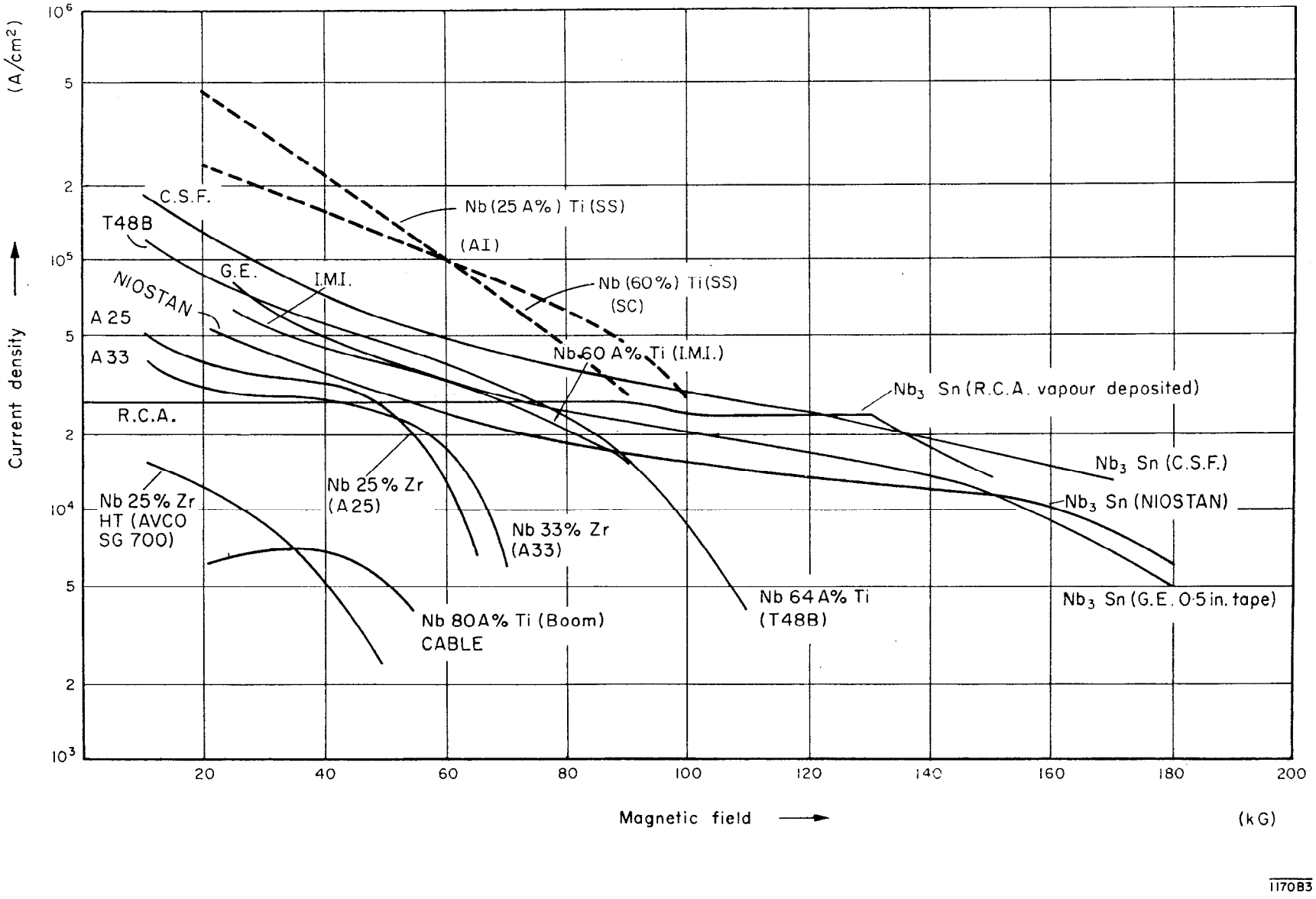
Current density (A/cm²)
10⁶
5
2
10⁵
5
2
10⁴
5
2
10³
20
40
60
80
100
120
140
160
180
200
Magnetic field (kG)
C.S.F.
T48B
NIOSTAN
A 25
A 33
R.C.A.
G.E.
I.M.I.
Nb (25 A%) Ti (SS)
(AI)
Nb (60%) Ti (SS)
(SC)
Nb 60 A% Ti (I.M.I.)
Nb₃ Sn (R.C.A. vapour deposited)
Nb₃ Sn (C.S.F.)
Nb₃ Sn (NIOSTAN)
Nb₃ Sn (G.E. 0·5 in. tape)
Nb 25% Zr
HT (AVCO
SG 700)
Nb 25% Zr
(A 25)
Nb 33% Zr
(A33)
Nb 80A% Ti (Boom)
CABLE
Nb 64 A% Ti
(T48B)
1170B3

Fig. 7

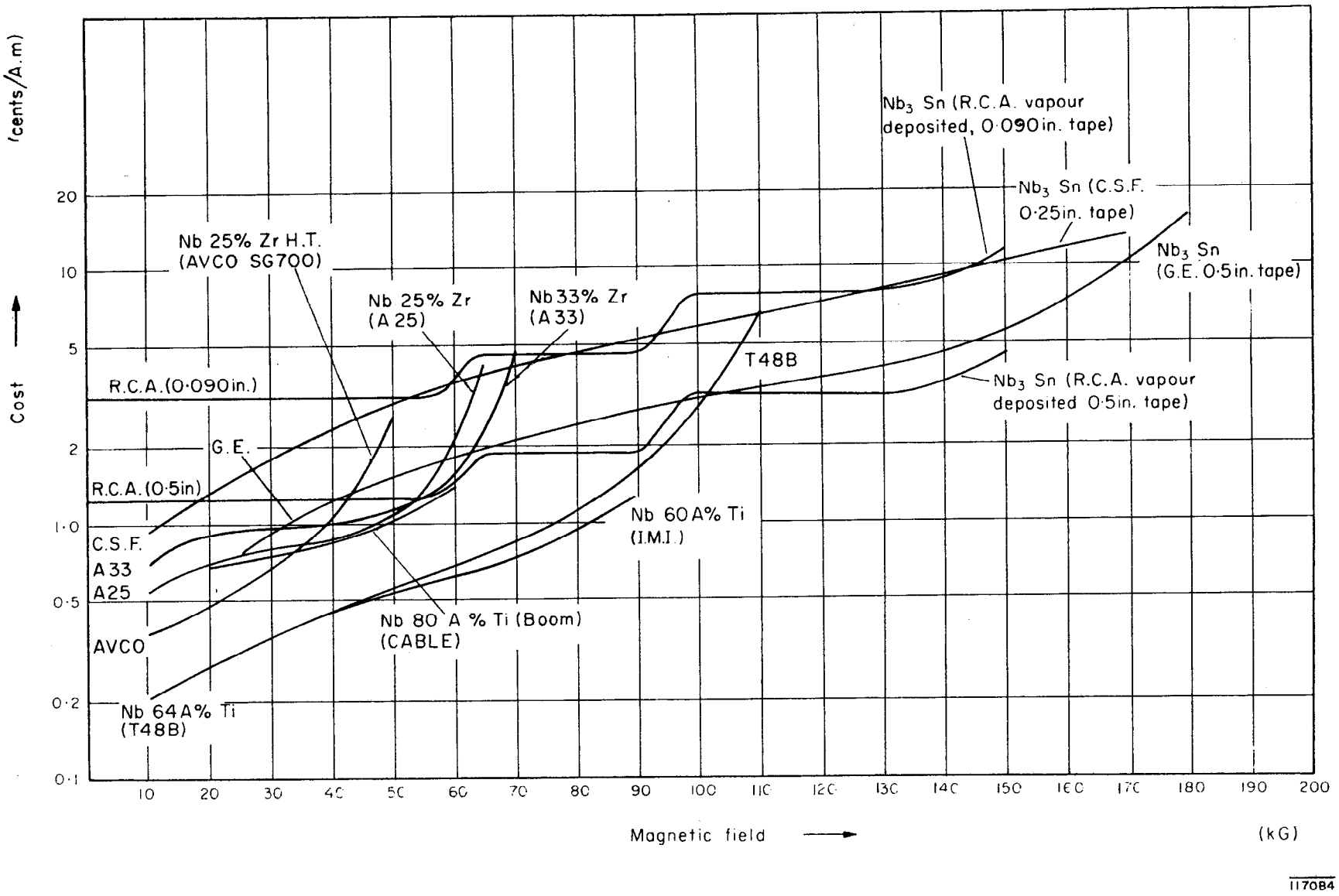
(cents/A.m)
Cost
20
10
5
2
1·0
0·5
0·2
0·1
Nb 25% Zr H.T.
(AVCO SG700)
Nb 25% Zr
(A 25)
Nb 33% Zr
(A 33)
Nb3 Sn (R.C.A. vapour
deposited, 0·090in. tape)
Nb3 Sn (C.S.F.
0·25in. tape)
Nb3 Sn
(G.E. 0·5in. tape)
T48B
R.C.A.(0·090in.)
G.E.
R.C.A.(0·5in)
Nb3 Sn (R.C.A. vapour
deposited 0·5in. tape)
Nb 60A% Ti
(I.M.I.)
C.S.F.
A33
A25
AVCO
Nb 80 A % Ti (Boom)
(CABLE)
Nb 64A% Ti
(T48B)
10
20
30
40
50
60
70
80
90
100
110
120
130
140
150
160
170
180
190
200
Magnetic field
(kG)
117084

Fig. 8

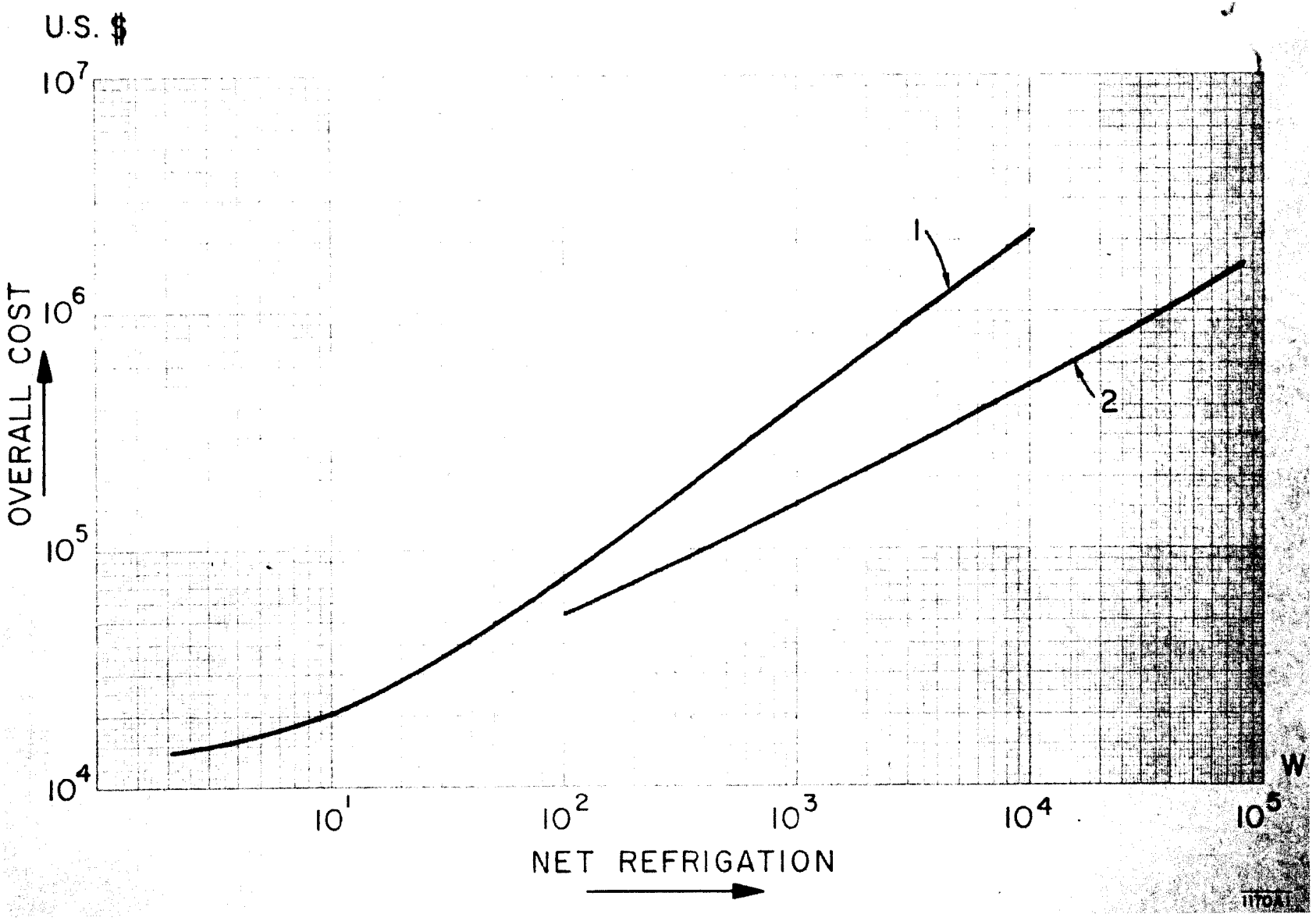
U.S. $
10^7
10^6
10^5
10^4
OVERALL COST
1
2
10^1
10^2
10^3
10^4
10^5
W
NET REFRIGATION
1170A1

Fig. 9

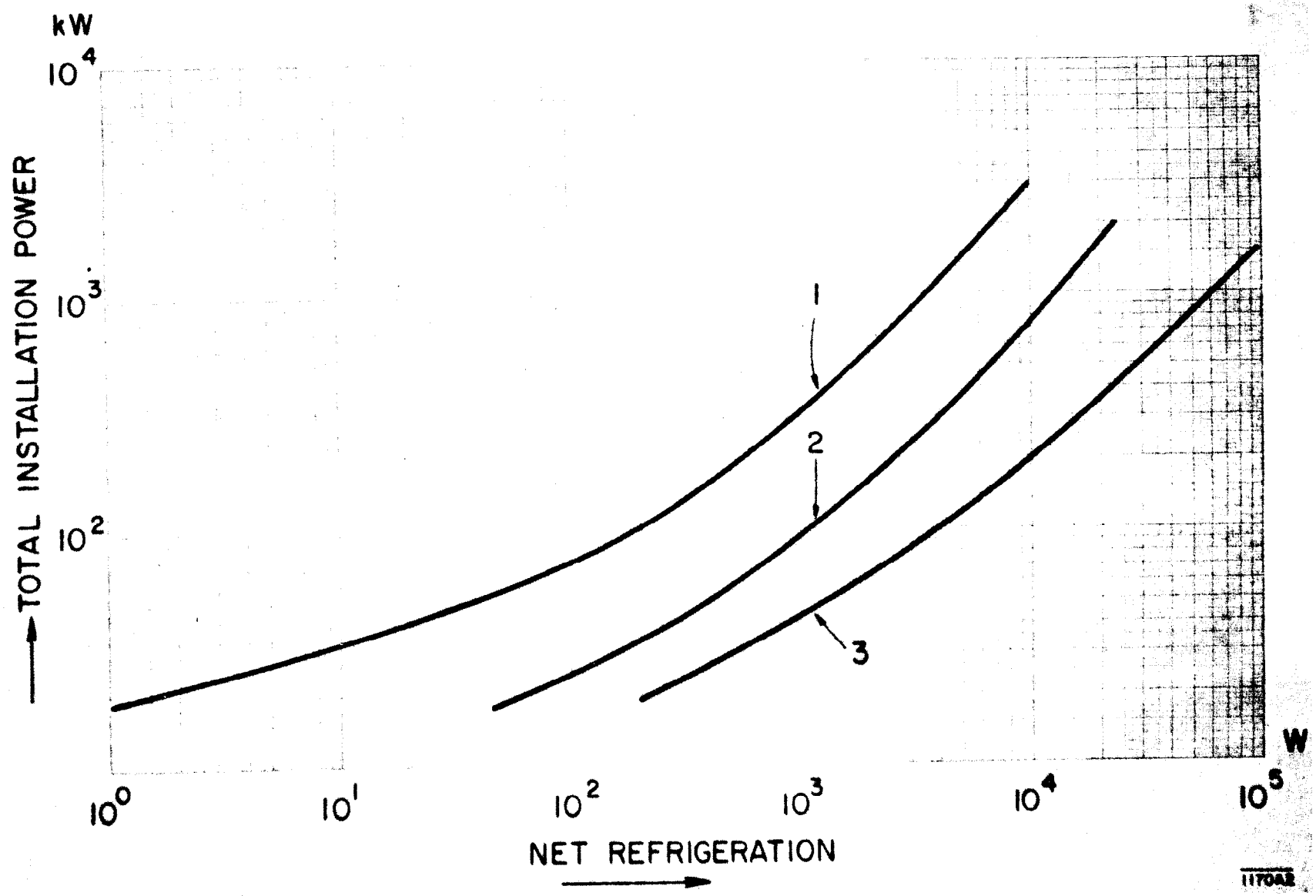
kW
10^4
10^3
10^2
TOTAL INSTALLATION POWER
1
2
3
10^0
10^1
10^2
10^3
10^4
10^5
W
NET REFRIGERATION
11704A

Fig. 10

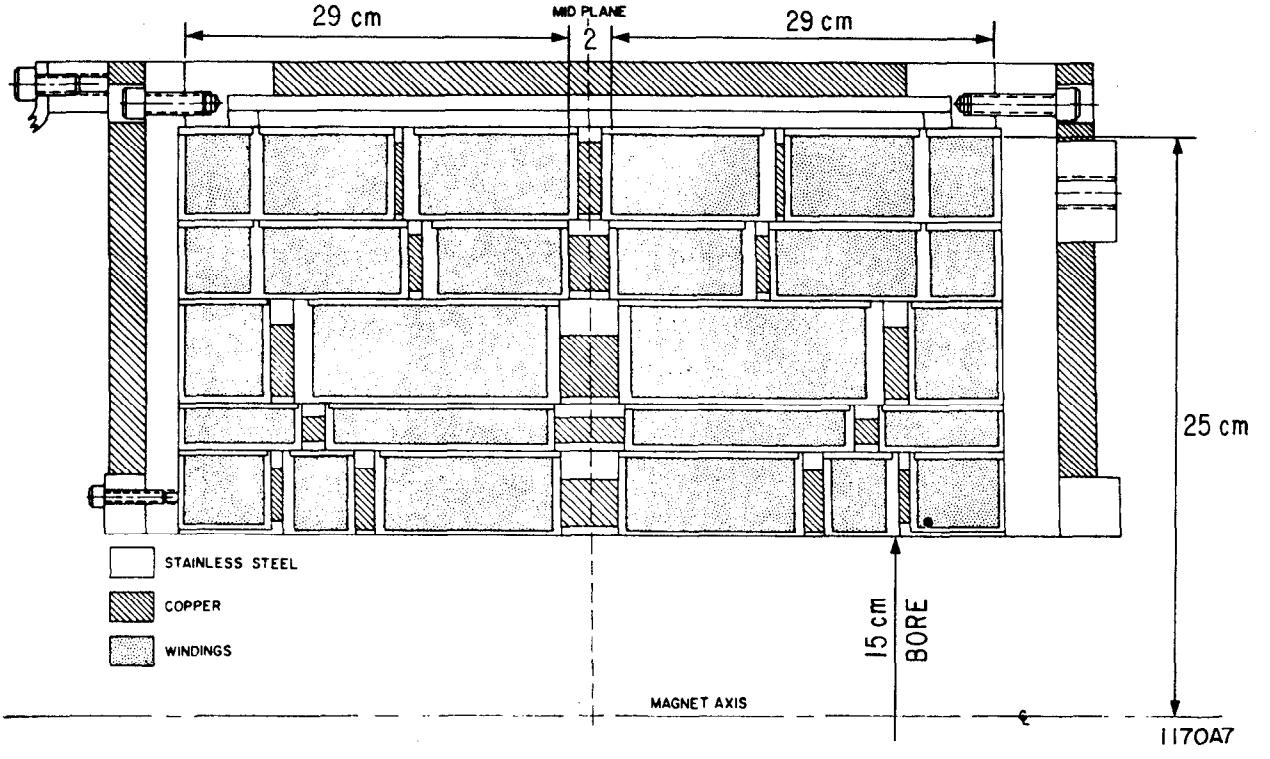
29 cm
MID PLANE
29 cm
25 cm
STAINLESS STEEL
COPPER
WINDINGS
15 cm
BORE
MAGNET AXIS
1170A7

Fig. 11

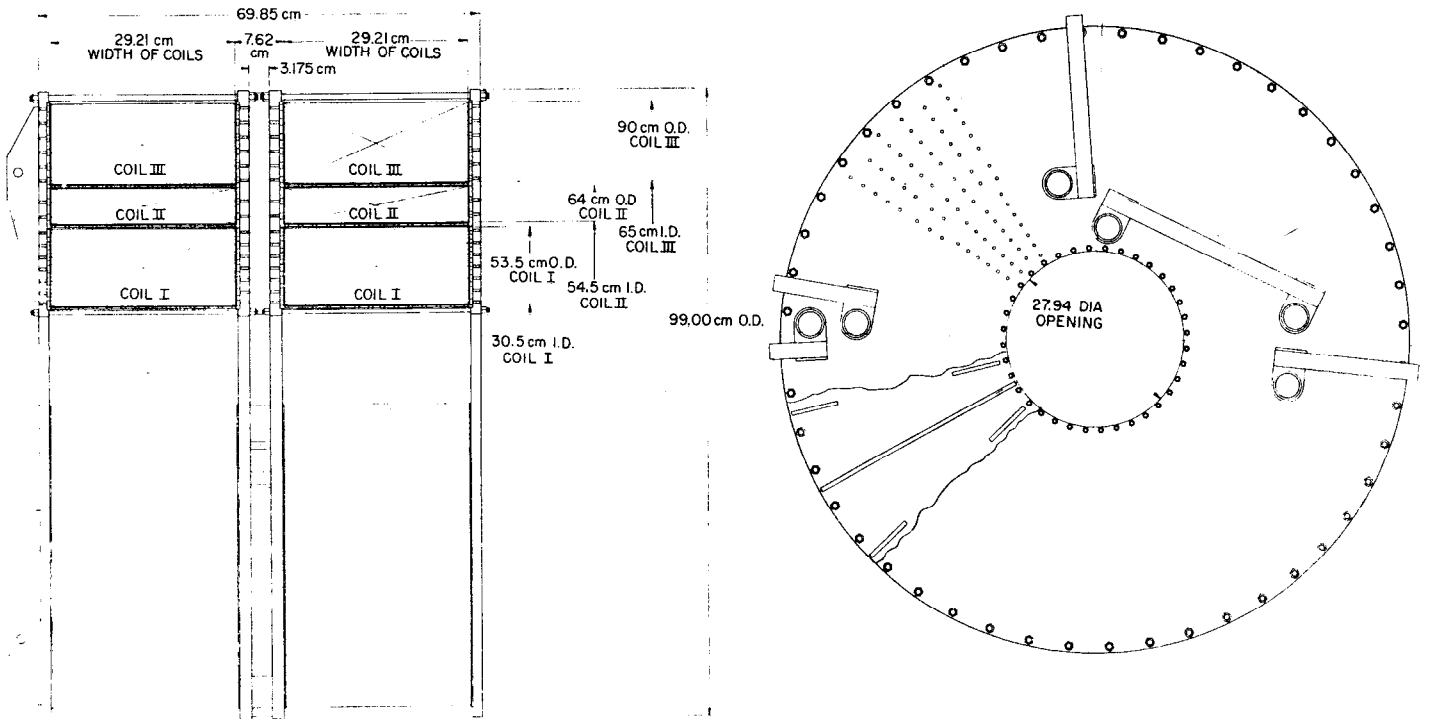

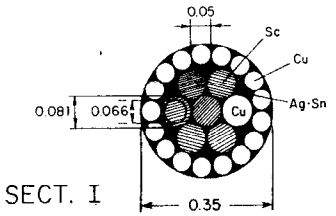

SECT. I

CABLE FOR COIL I

36 LAYERS WITH 72 TURNS/LAYER

≅ 2600 TURNS

$I_{av} = 3.16 \times 10^3\ Acm^{-2}$

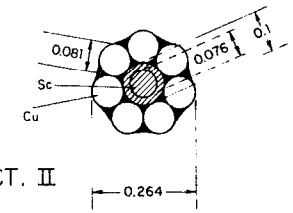

SECT. II

CABLE FOR COIL II

16 LAYERS WITH 88 TURNS/LAYER

≅ 1400 TURNS

$I_{av} = 4.84 \times 10^3\ Acm^{-2}$

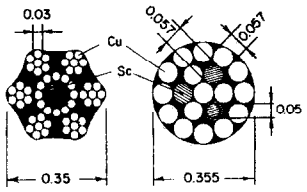

SECT. III

CABLE FOR COIL III

34 LAYERS WITH 76 TURNS/LAYER

≅ 2500 TURNS

$I_{av} = 3.36 \times 10^3\ Acm^{-2}$

507-15-C

Fig. 12

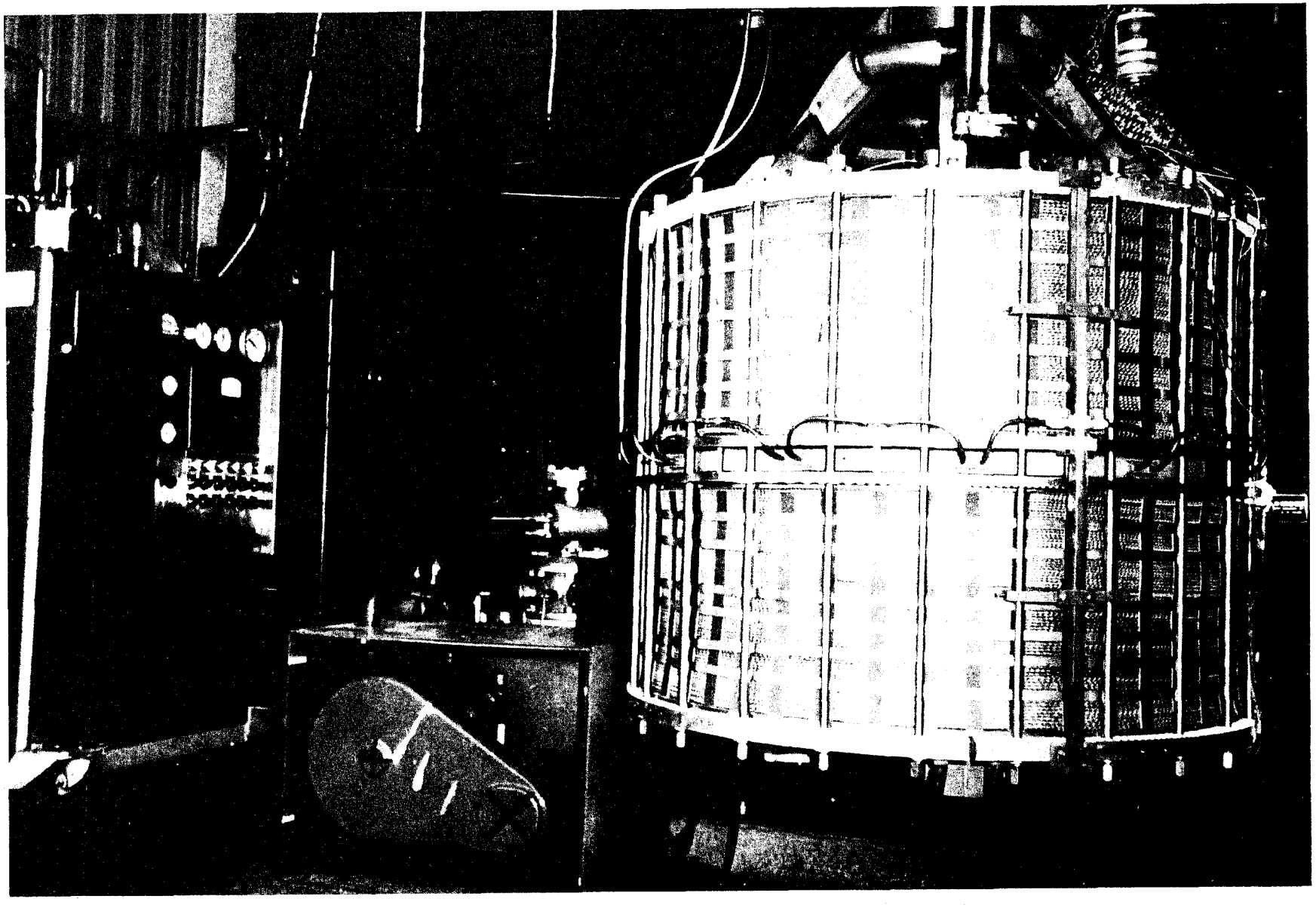

Fig. 13

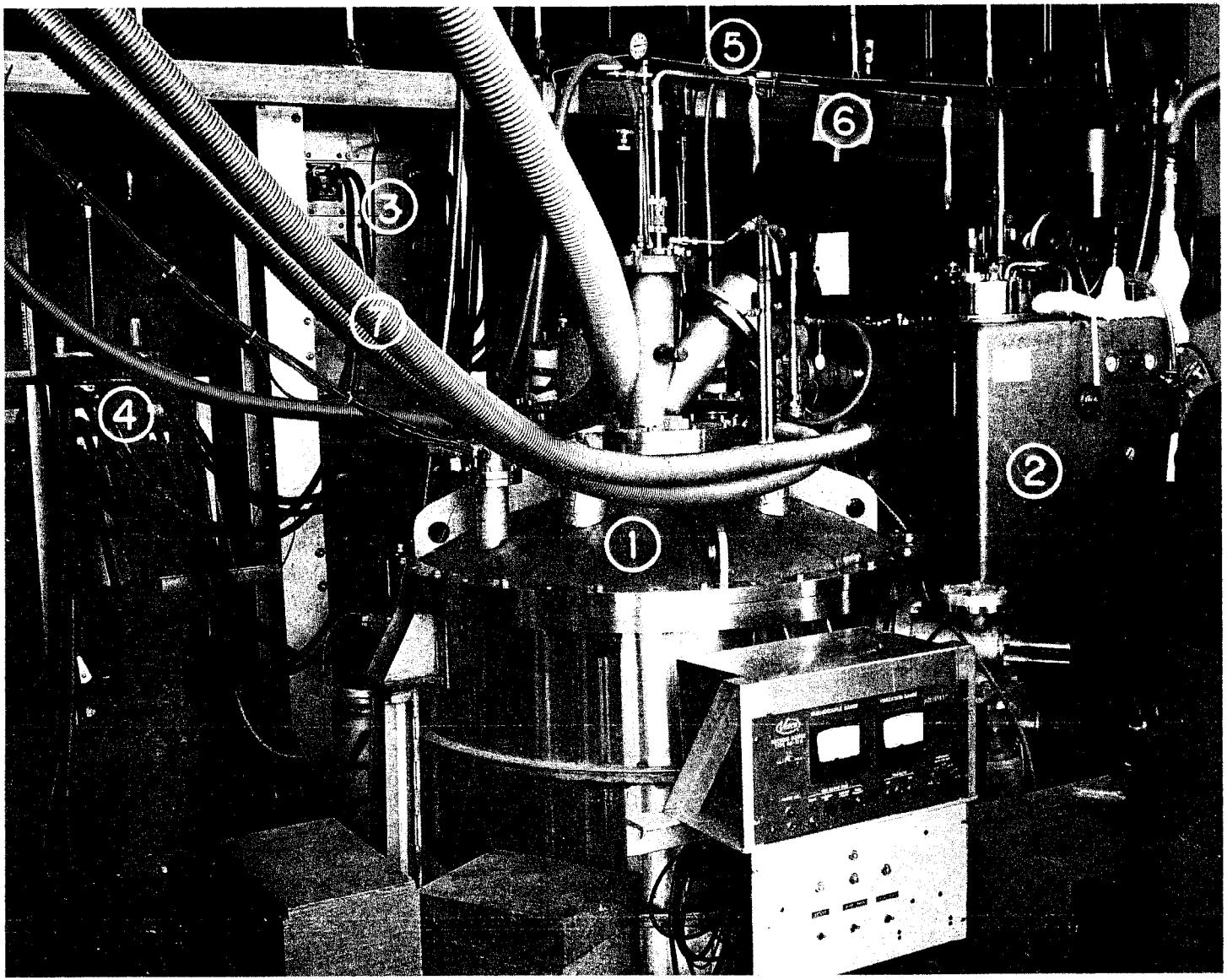

1170A9

Fig. 14

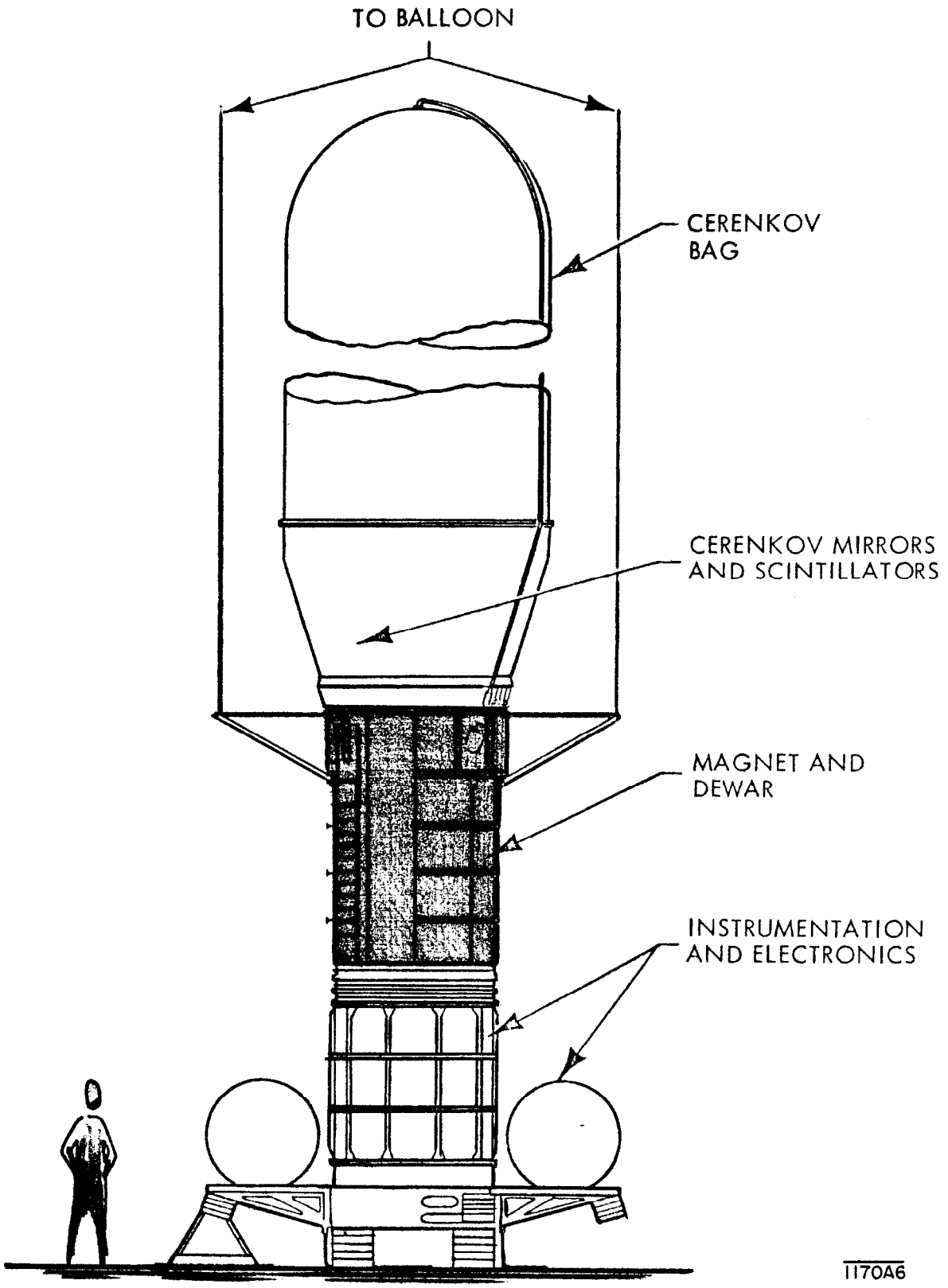
TO BALLOON
CERENKOV BAG
CERENKOV MIRRORS AND SCINTILLATORS
MAGNET AND DEWAR
INSTRUMENTATION AND ELECTRONICS
1170A6

Fig. 15

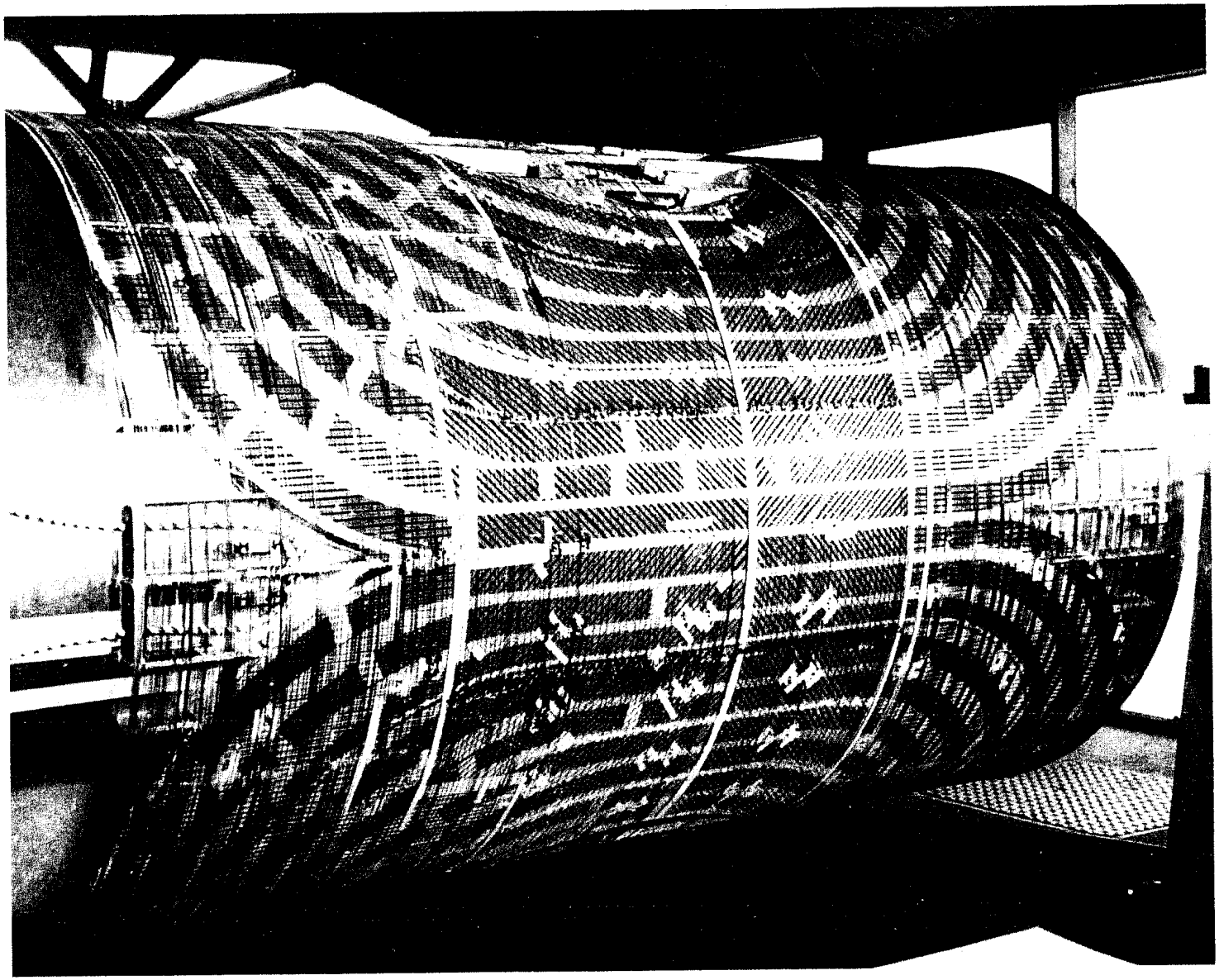

Fig. 16

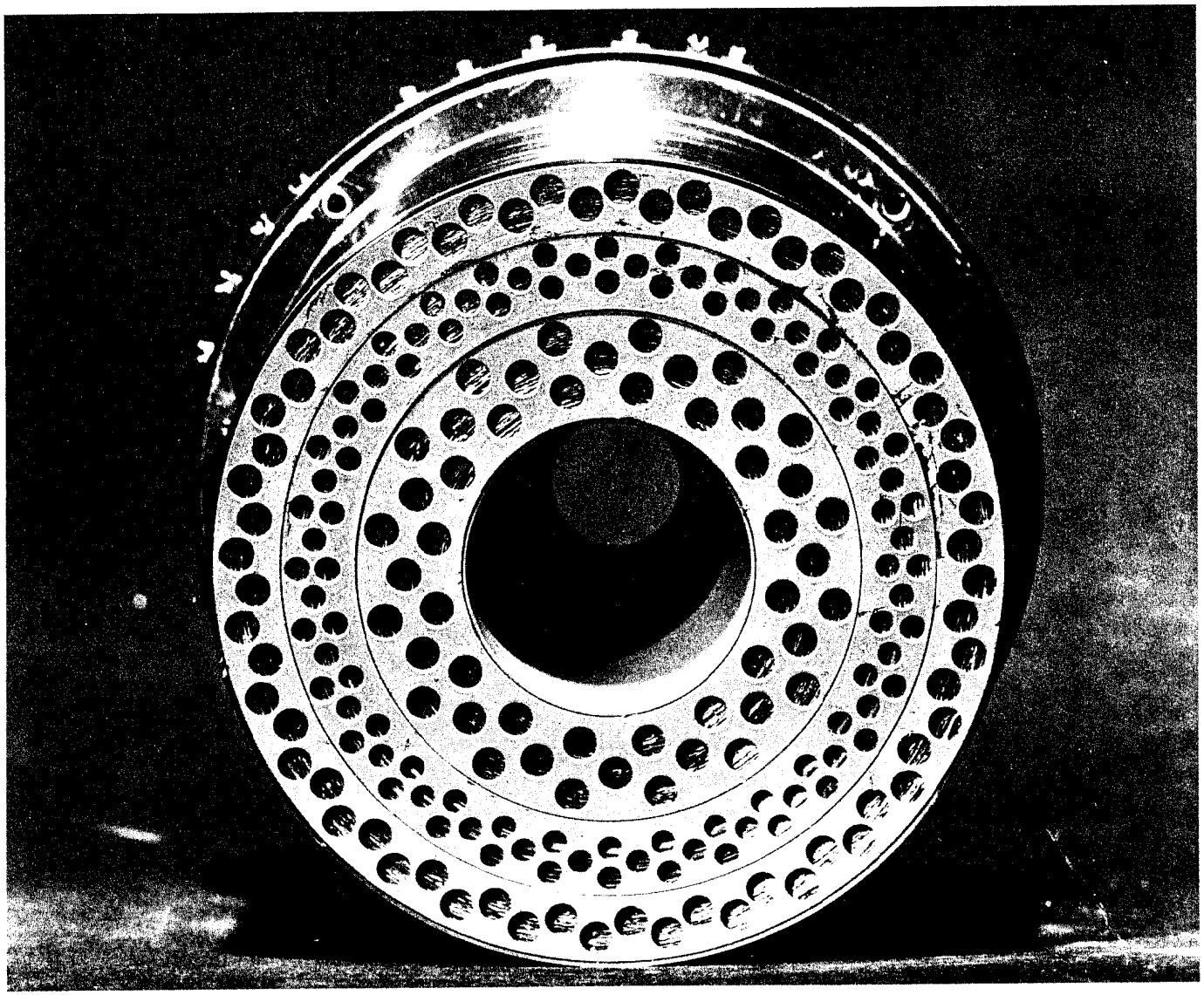

Fig. 17

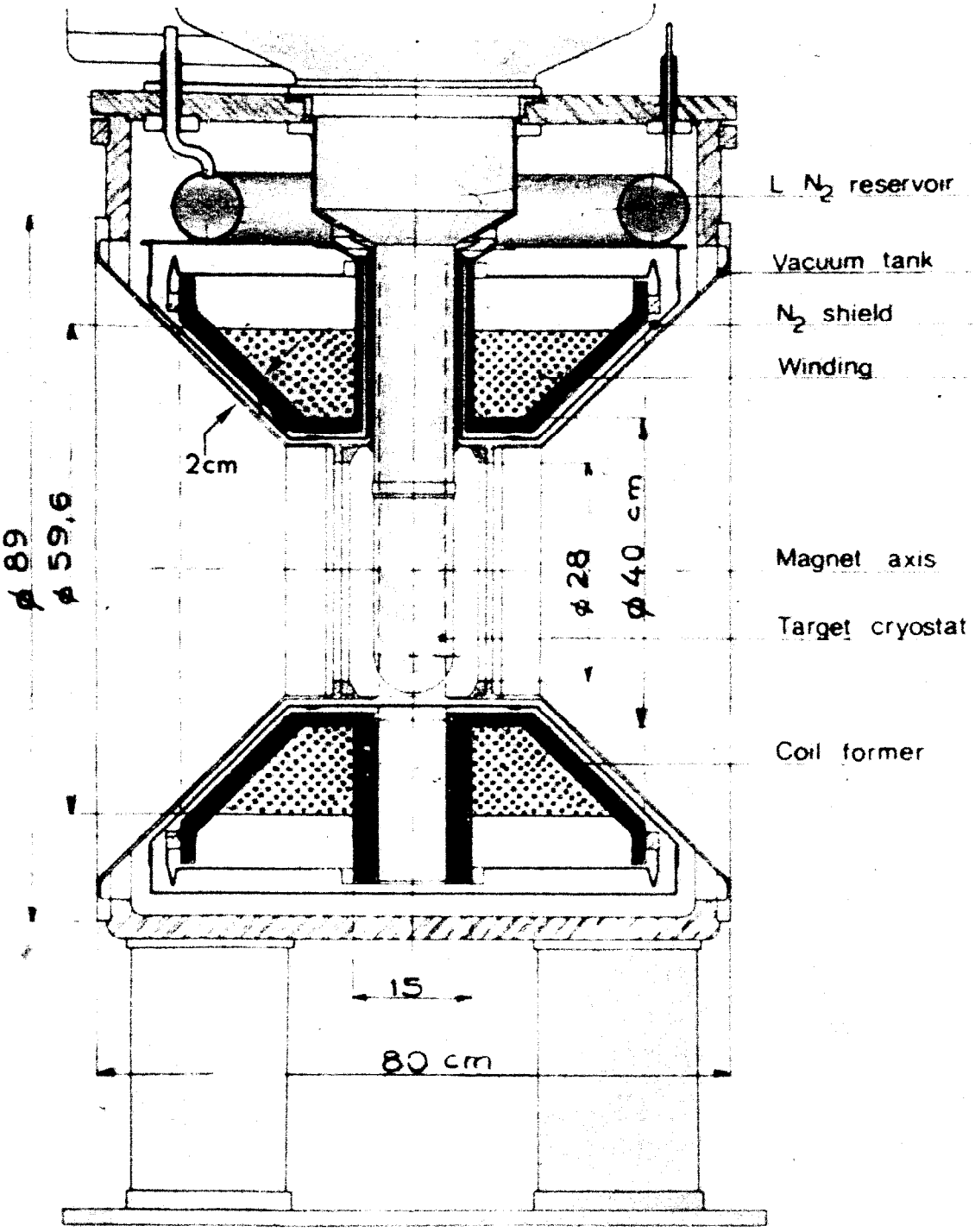
L N_2 reservoir
Vacuum tank
N_2 shield
Winding
2cm
ϕ 89
ϕ 59,6
ϕ 28
ϕ 40 cm
Magnet axis
Target cryostat
Coil former
15
80 cm

Fig. 18

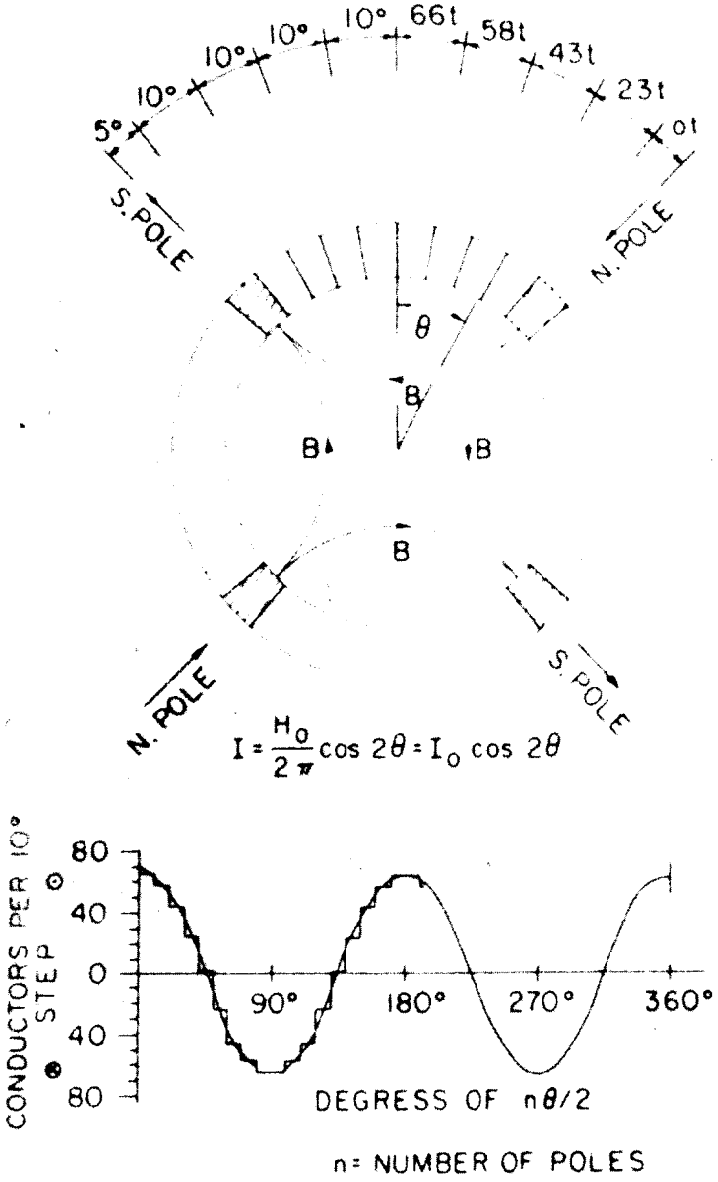

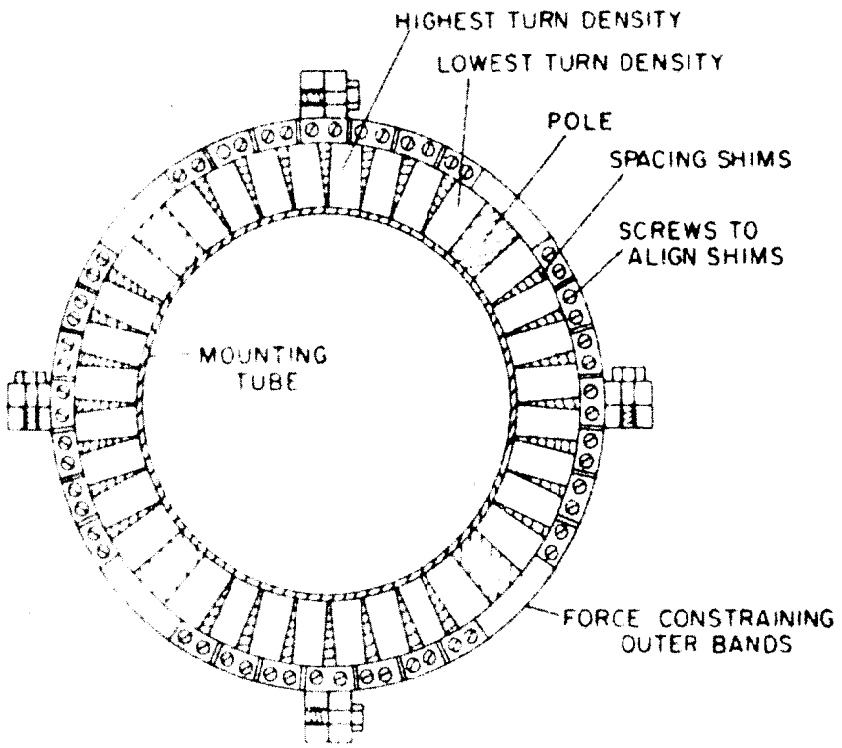

CROSS SECTIONAL VIEW OF SUPERCONDUCTING QUADRUPOLE

Fig. 19

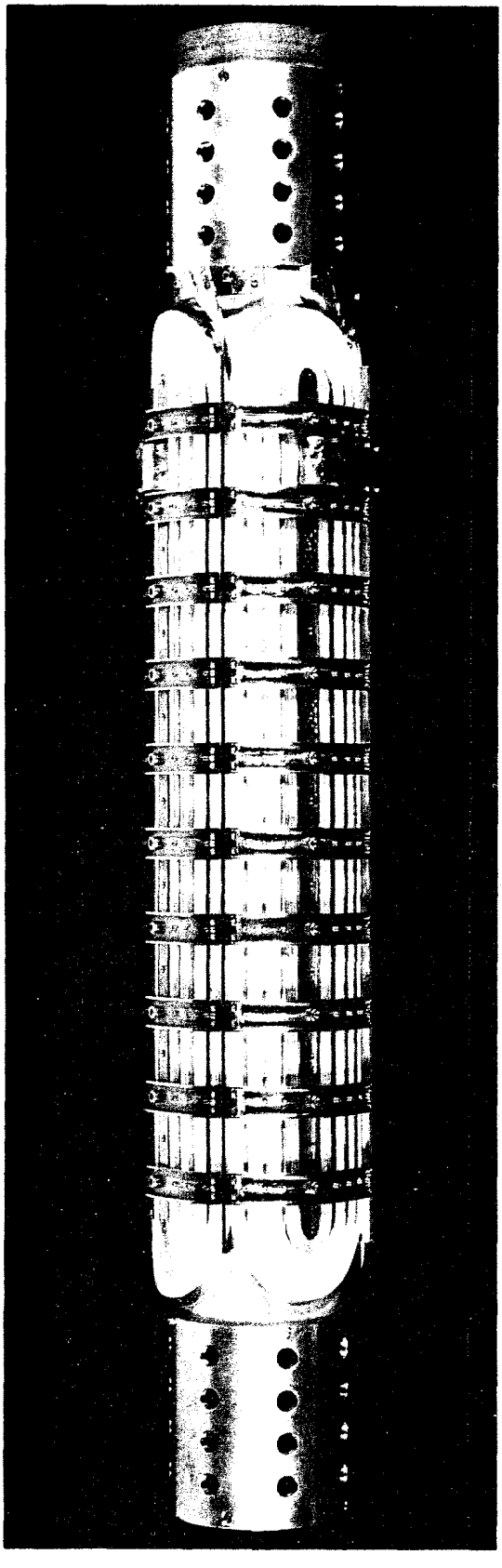

Fig. 20

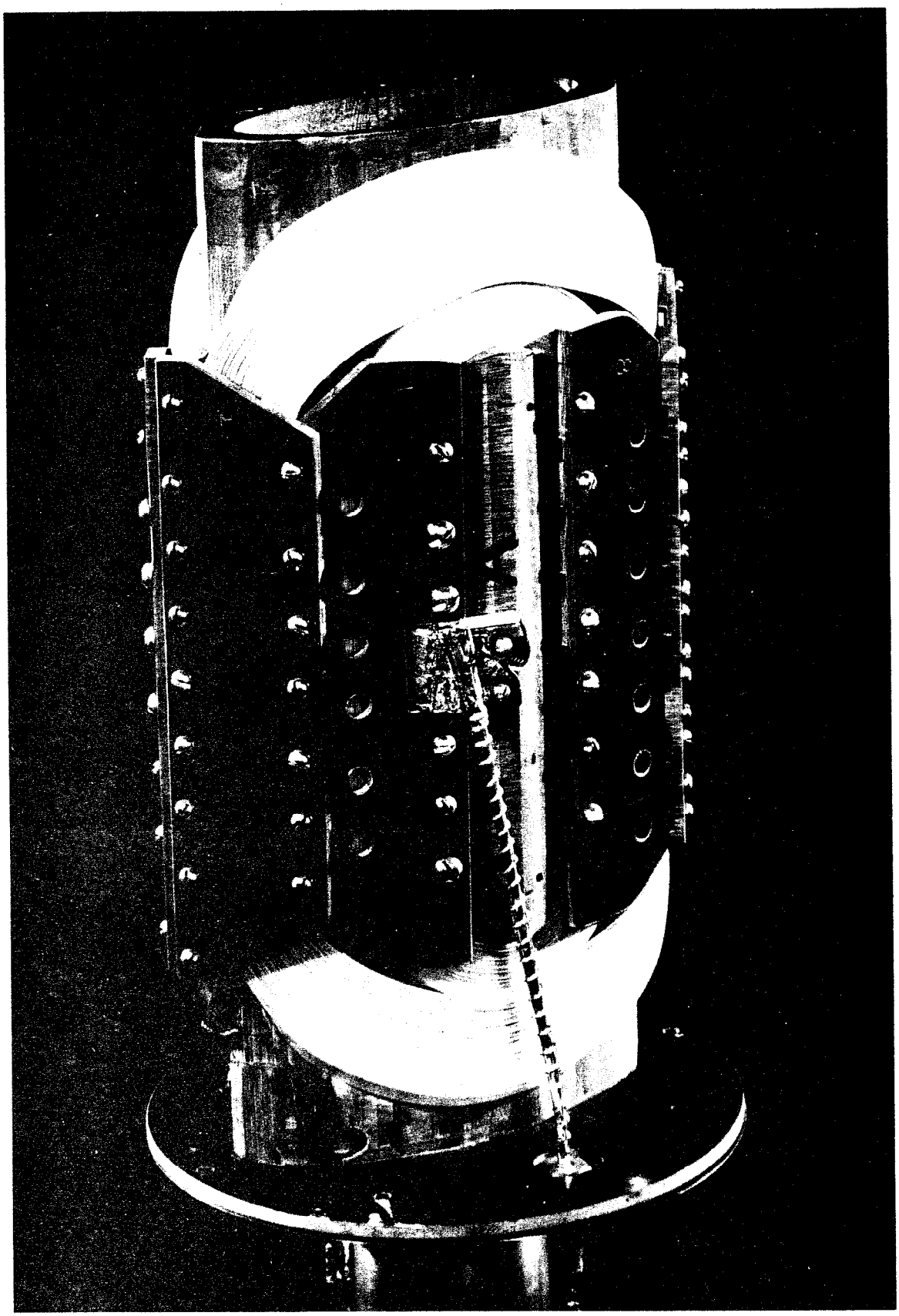

Fig. 21

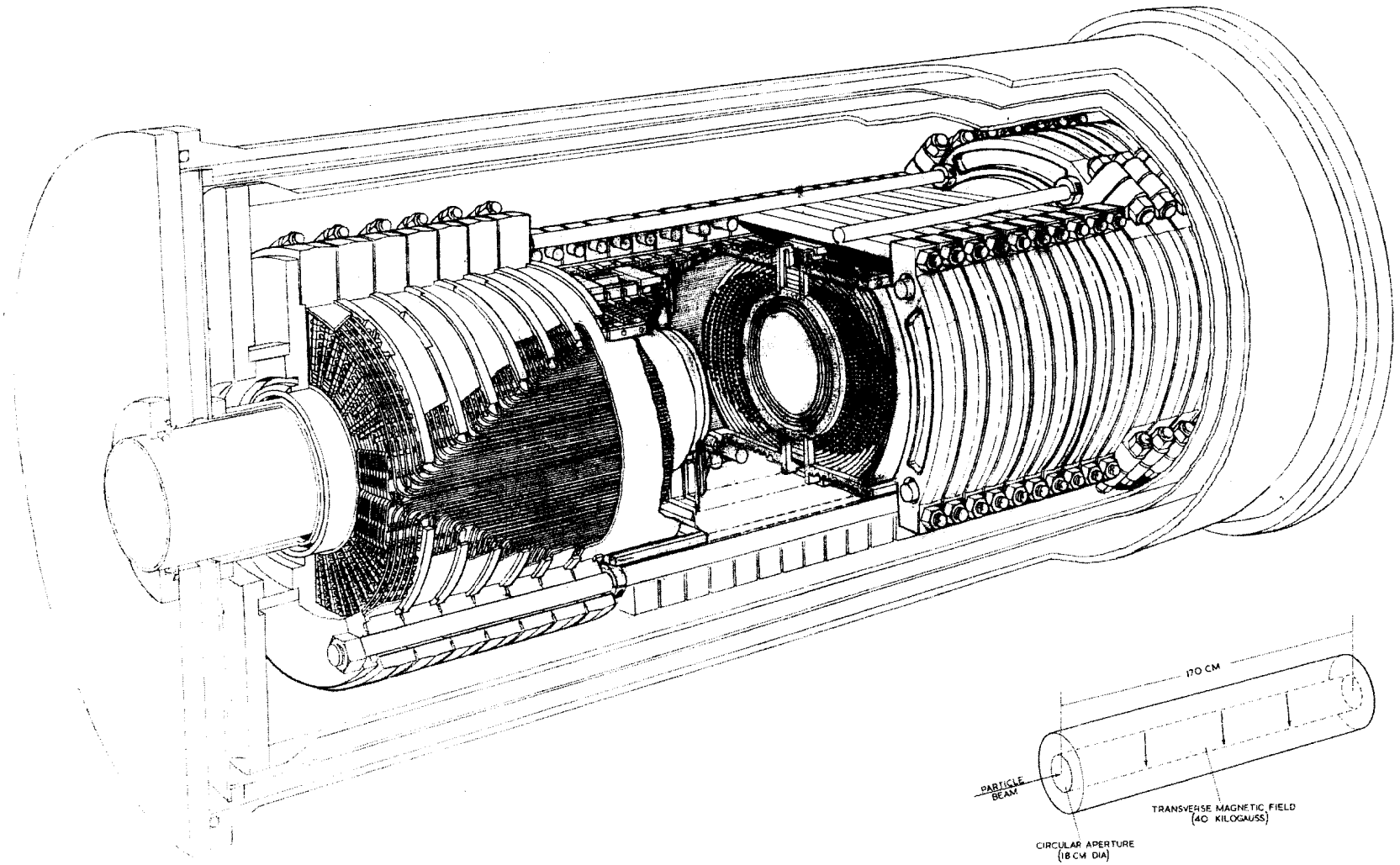

SUPERCONDUCTING BENDING MAGNET

Fig. 22

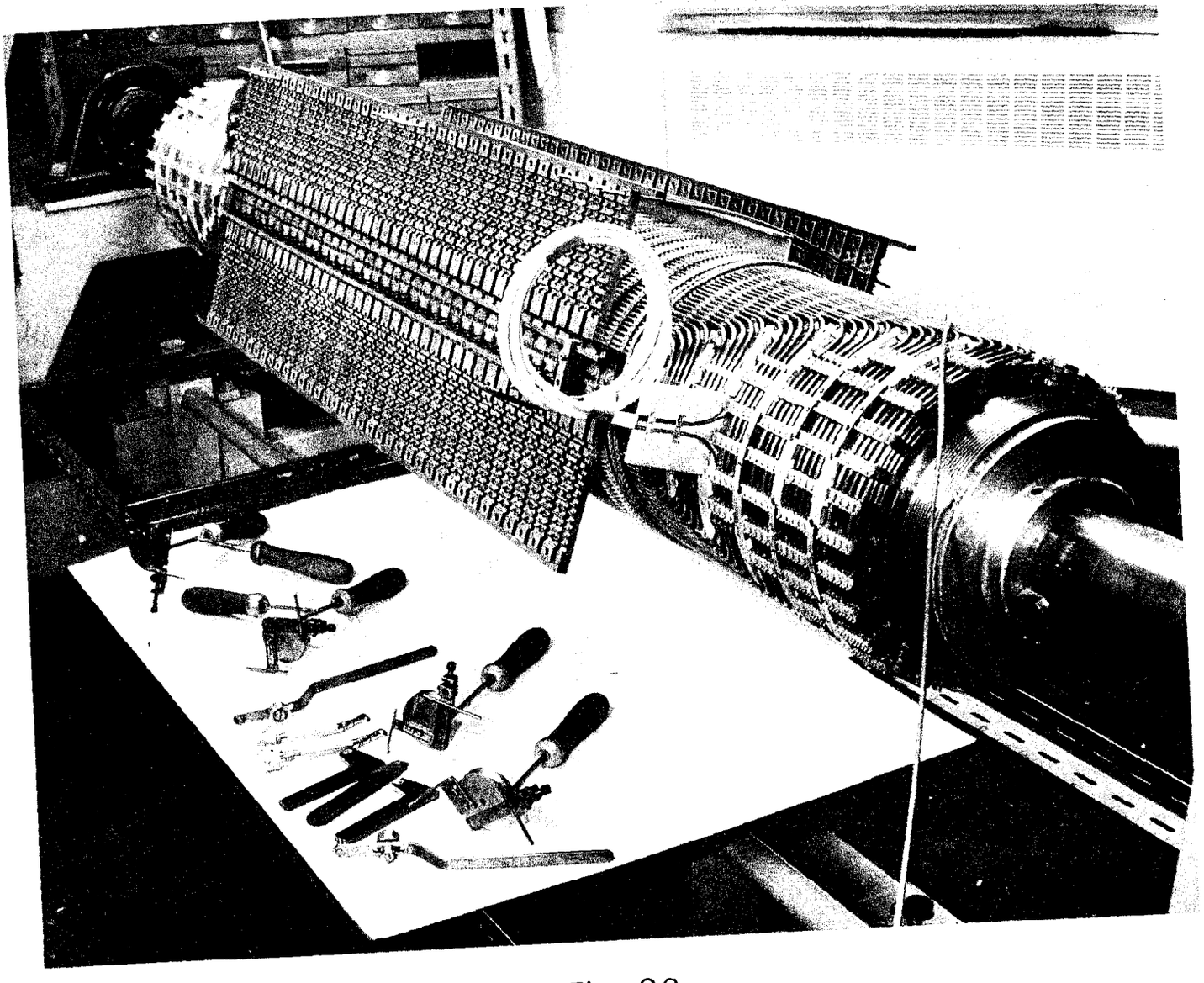

Fig. 23

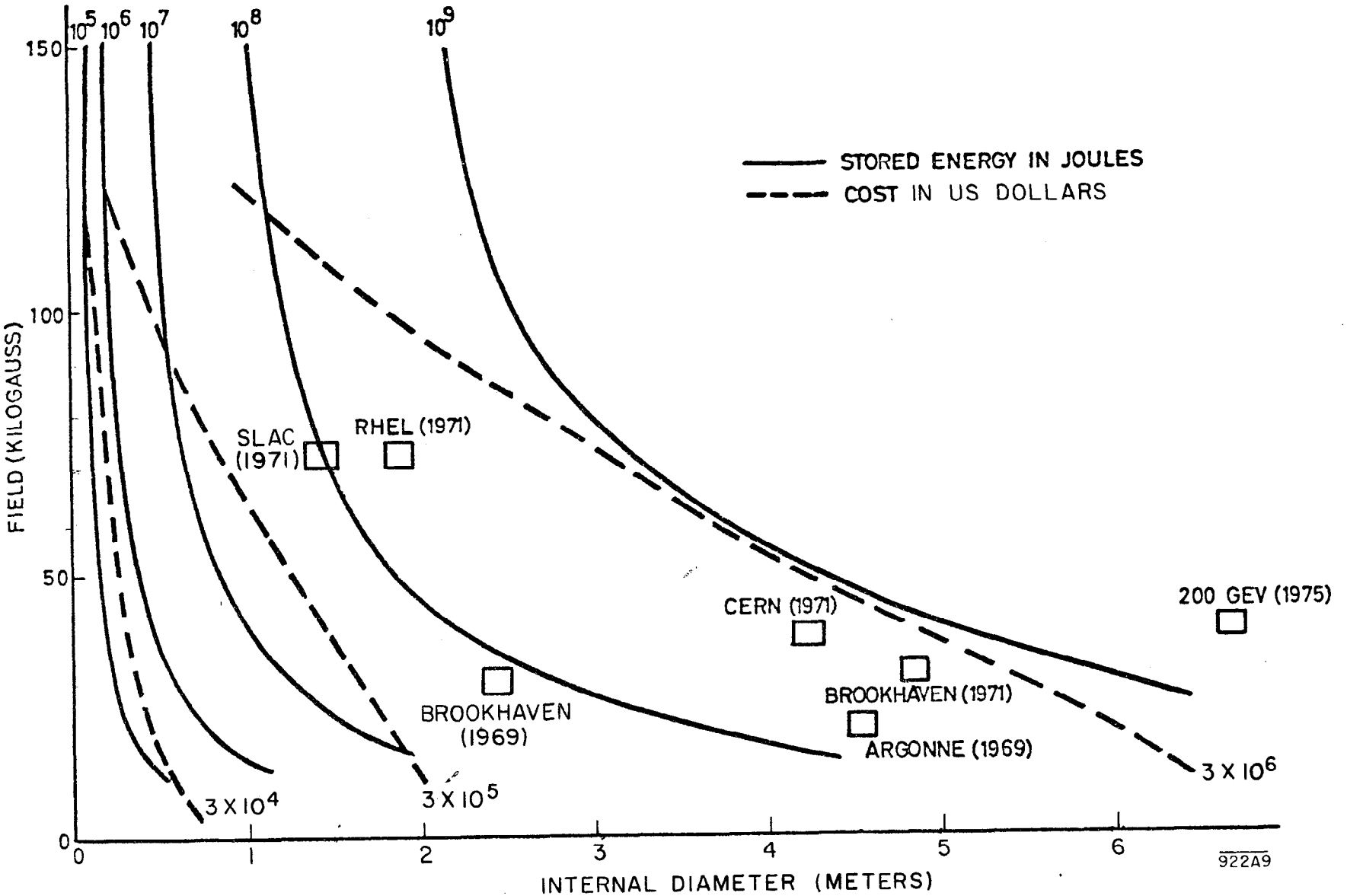
STORED ENERGY IN JOULES
COST IN US DOLLARS
10^5
10^6
10^7
10^8
10^9
150
100
50
0
FIELD (KILOGAUSS)
SLAC (1971)
RHEL (1971)
CERN (1971)
200 GEV (1975)
BROOKHAVEN (1969)
BROOKHAVEN (1971)
ARGONNE (1969)
3×10^4
3×10^5
3×10^6
0
1
2
3
4
5
6
INTERNAL DIAMETER (METERS)
922A9

Fig. 24

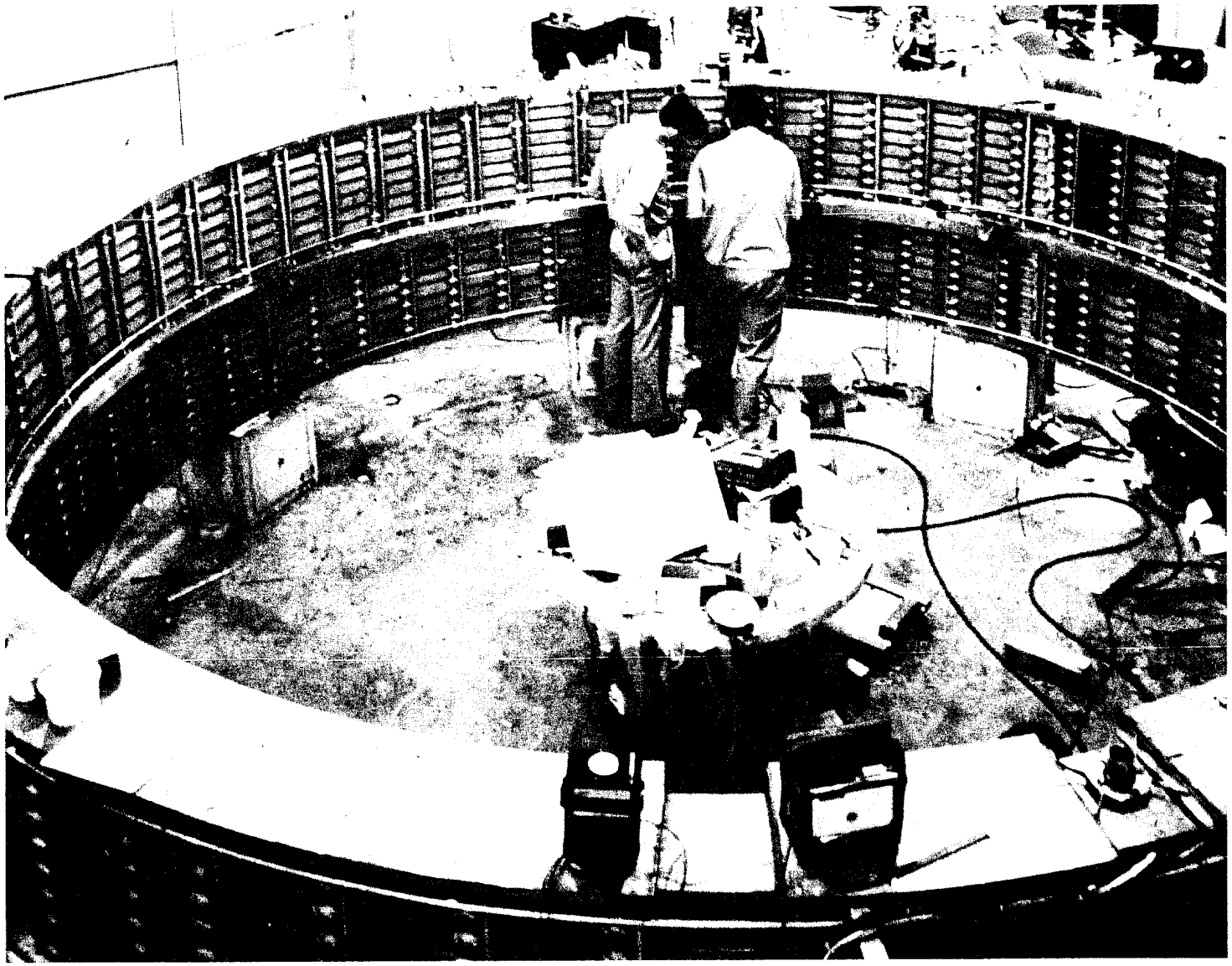

Fig. 25

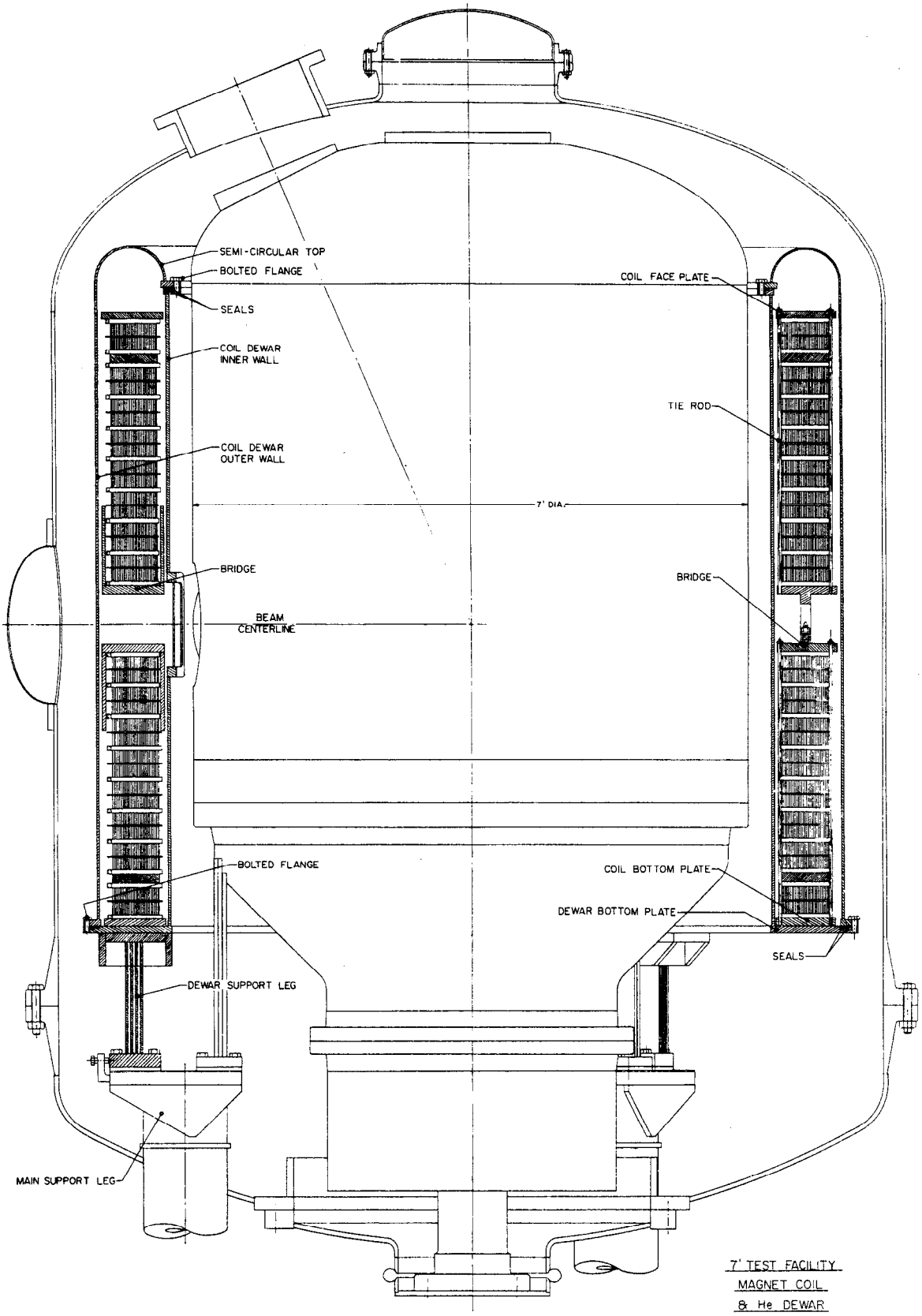
SEMI-CIRCULAR TOP
BOLTED FLANGE
SEALS
COIL DEWAR INNER WALL
COIL DEWAR OUTER WALL
BRIDGE
BEAM CENTERLINE
BOLTED FLANGE
DEWAR SUPPORT LEG
MAIN SUPPORT LEG
COIL FACE PLATE
TIE ROD
7' DIA.
BRIDGE
COIL BOTTOM PLATE
DEWAR BOTTOM PLATE
SEALS
7' TEST FACILITY
MAGNET COIL
& He DEWAR

Fig. 26

Fig. 27

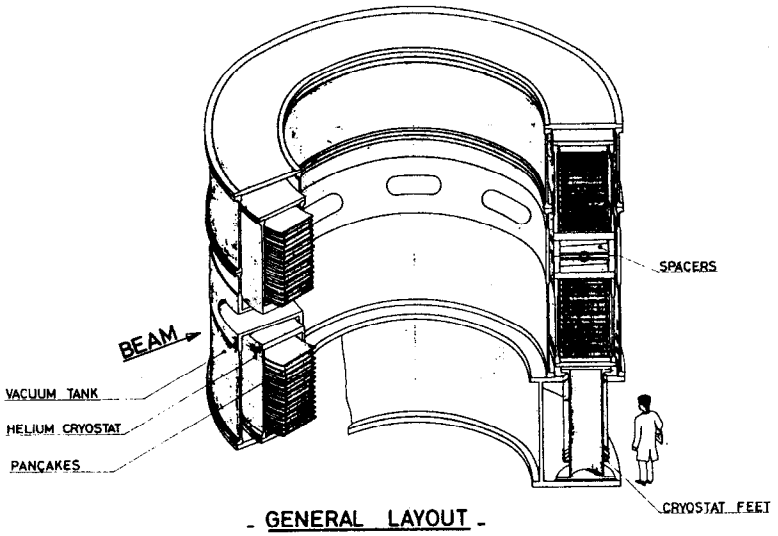

- GENERAL LAYOUT -

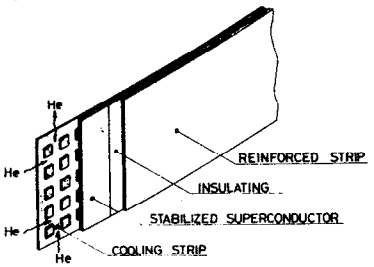

- DETAIL OF THE CONDUCTOR -

MAGNET PARAMETERS

CENTRAL FIELD	35 000 G
MAXIMUM FIELD ON THE CONDUCTOR	51000 G
RATED CURRENT	5700A
STORED ENERGY	750 M. Joules
ATTRACTIVE FORCES	9000 Tonnes
WEIGHT OF SUPERCONDUCTING MATERIAL	3 Tonnes
WEIGHT OF COPPER	96 Tonnes

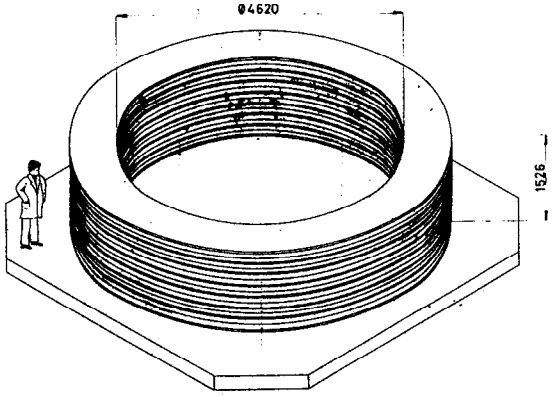

- COIL -

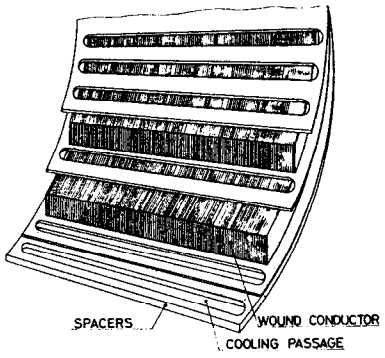

- DETAIL OF A PANCAKE -

Fig. 28

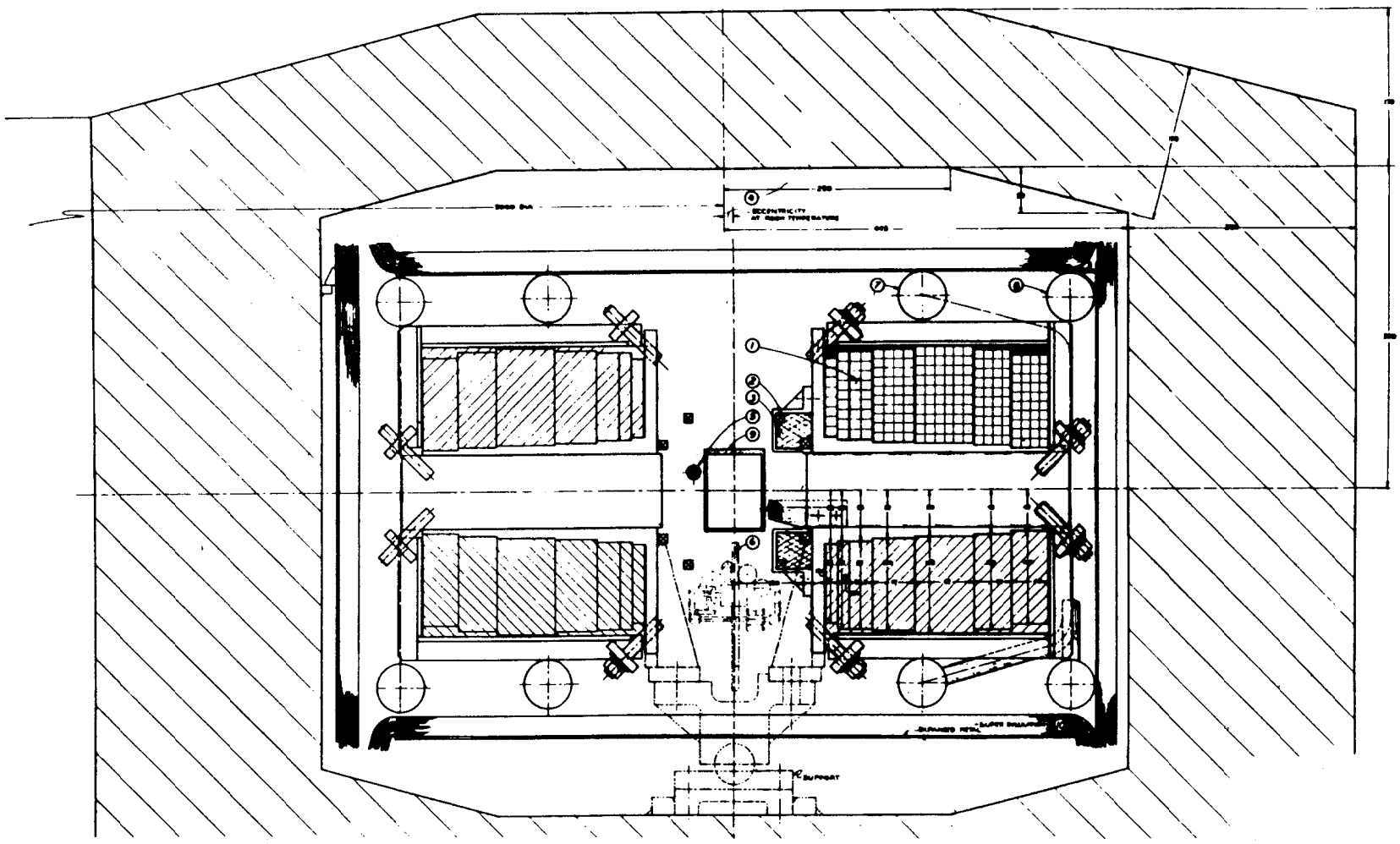

Fig. 29

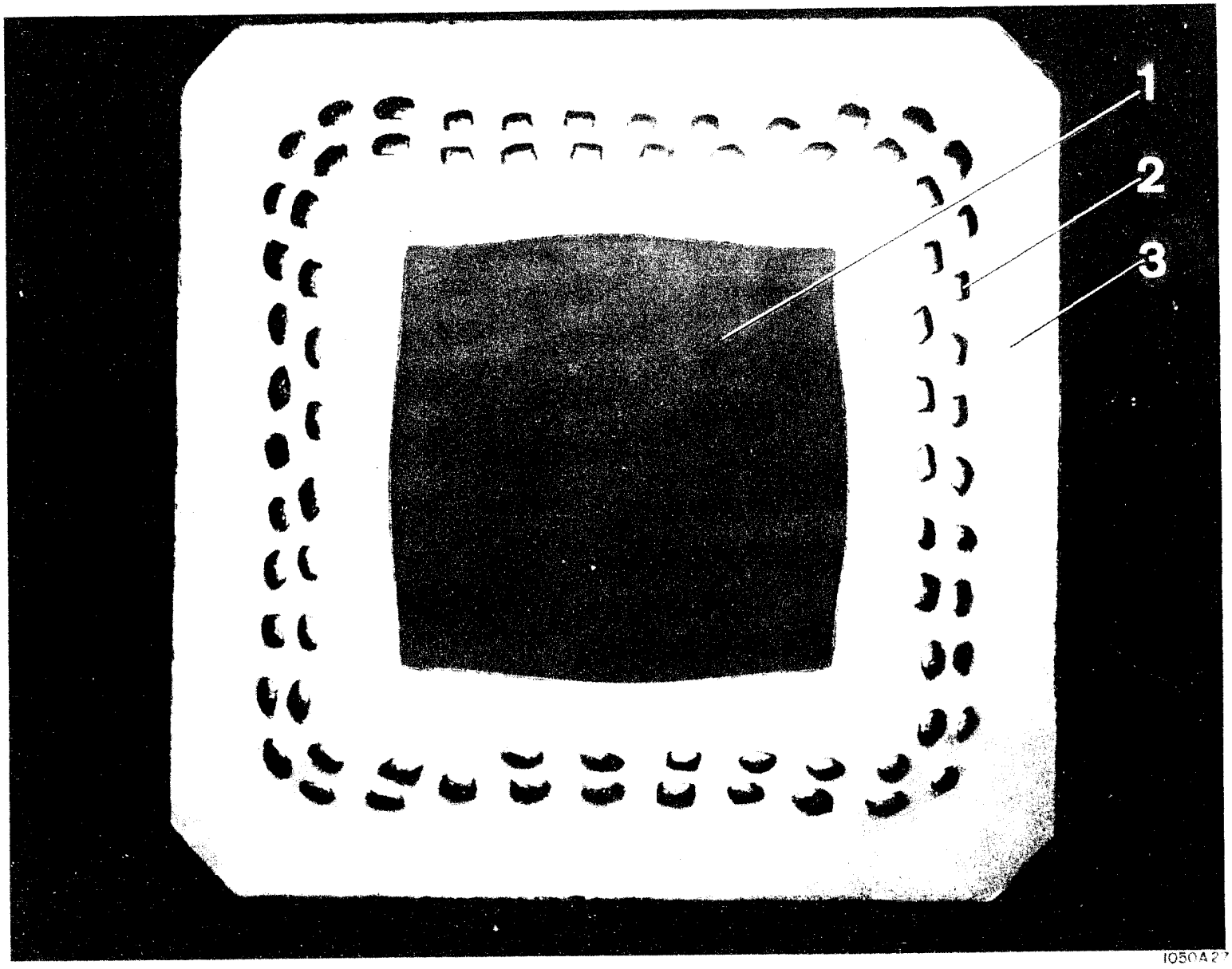

Fig. 30

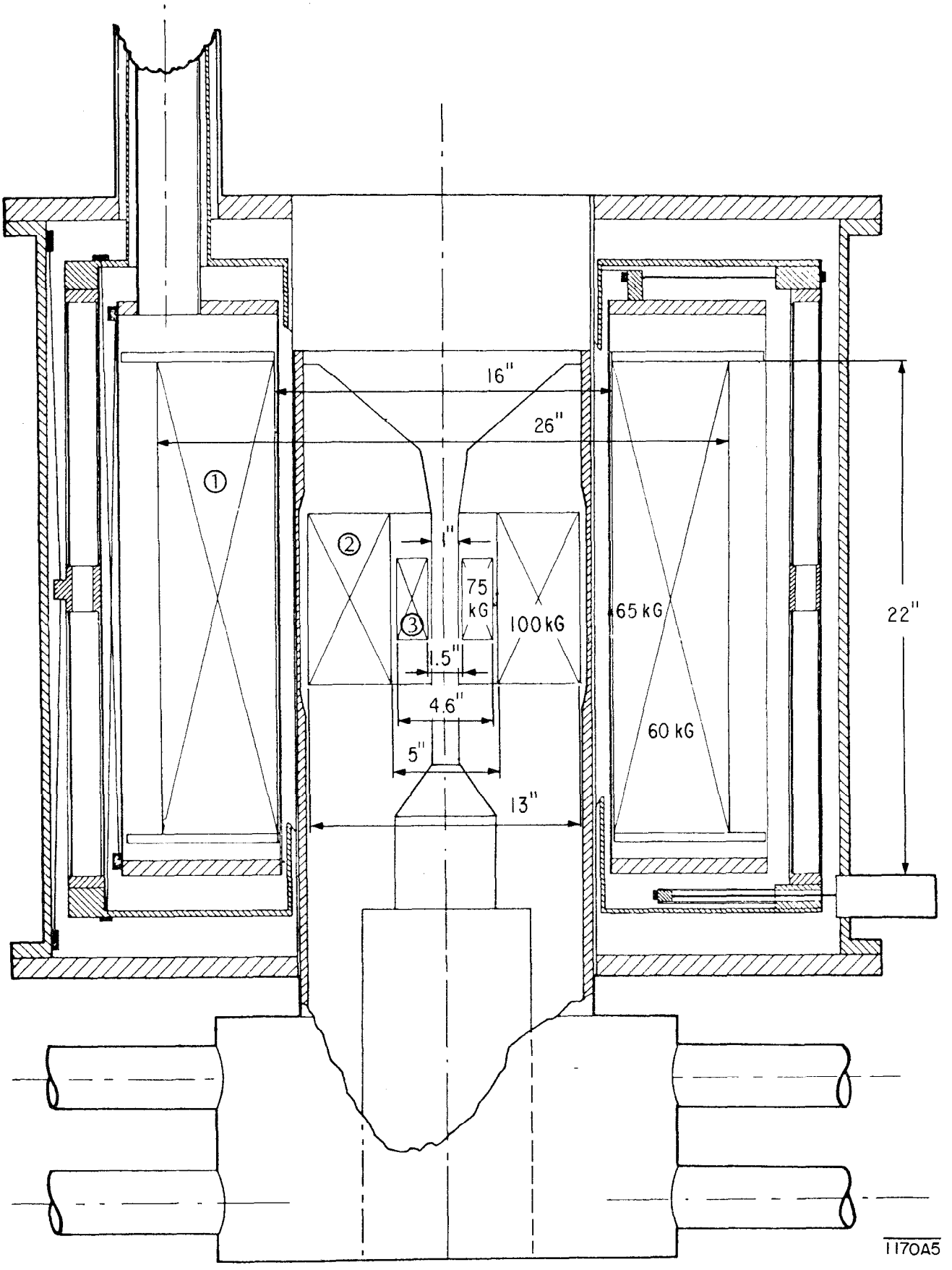

Fig. 31